Since January 2020 Elsevier has created a COVID-19 resource centre with free information in English and Mandarin on the novel coronavirus COVID-19. The COVID-19 resource centre is hosted on Elsevier Connect, the company's public news and information website.

Biosensors and Bioelectronics 166 (2020) 112455

Contents lists available at ScienceDirect

Biosensors and Bioelectronics

journal homepage: http://www.elsevier.com/locate/bios

Detection of COVID-19: A review of the current literature and future perspectives

Tianxing Ji [a,*,1], Zhenwei Liu [b,1], GuoQiang Wang [c,1], Xuguang Guo [d,1], Shahzad Akbar khan [e], Changchun Lai [f], Haoyu Chen [a], Shiwen Huang [a], Shaomei Xia [a], Bo Chen [a], Hongyun Jia [a], Yangchao Chen [g,***], Qiang Zhou [a,**]

[a] Department of Clinical Laboratory Medicine, The Second Affiliated Hospital of Guangzhou Medical University, Guangzhou, 510260, PR China
[b] Guangzhou Institute of Respiratory Medicine Company Limited, Guangzhou, 510535, PR China
[c] Department of Gastrointestinal Surgery, The Second Affiliated Hospital of Guangzhou Medical University, Guangzhou, 510260, PR China
[d] Department of Clinical Laboratory Medicine, The Third Affiliated Hospital of Guangzhou Medical University, Guangzhou, 510150, PR China
[e] Laboratory of Pathology, Department of Pathobiology, University of Poonch Rawalakot, Rawala Kot, 12350, Pakistan
[f] Department of Clinical Laboratory, Maoming People's Hospital, Maoming, 525000, PR China
[g] School of Biomedical Sciences, Faculty of Medicine, The Chinese University of Hong Kong, Shatin, HongKong, PR China

ARTICLE INFO

Keywords:
Point-of-care testing
COVID-19
SARS-CoV-2

ABSTRACT

The rapid spread of severe acute respiratory syndrome coronavirus 2 (SARS-CoV-2) has led to the coronavirus disease 2019 (COVID-19) worldwide pandemic. This unprecedented situation has garnered worldwide attention. An effective strategy for controlling the COVID-19 pandemic is to develop highly accurate methods for the rapid identification and isolation of SARS-CoV-2 infected patients. Many companies and institutes are therefore striving to develop effective methods for the rapid detection of SARS-CoV-2 ribonucleic acid (RNA), antibodies, antigens, and the virus. In this review, we summarize the structure of the SARS-CoV-2 virus, its genome and gene expression characteristics, and the current progression of SARS-CoV-2 RNA, antibodies, antigens, and virus detection. Further, we discuss the reasons for the observed false-negative and false-positive RNA and antibody detection results in practical clinical applications. Finally, we provide a review of the biosensors which hold promising potential for point-of-care detection of COVID-19 patients. This review thereby provides general guidelines for both scientists in the biosensing research community and for those in the biosensor industry to develop a highly sensitive and accurate point-of-care COVID-19 detection system, which would be of enormous benefit for controlling the current COVID-19 pandemic.

1. Introduction

The recent emergence of the novel coronavirus (SARS-CoV-2, 2019-nCoV) which caused the coronavirus disease 2019 (COVID-19) outbreak in China has brought serious threats to public health worldwide (Wang et al., 2020). Although transportation to and from Wuhan and several other cities in China was closed from January 23, 2020, with the aim of reducing the virus transmission both in China and worldwide, as of July 4, 2020, there were 11,191,872 laboratory-confirmed SARS-CoV-2-infected cases and 529,122 reported deaths all over the world. (https://voice.baidu.com/act/newpneumonia/newpneumonia/?from=osari_pc_3#tab4). The increasing gravity of the situation could be related to a shortage of effective point-of-care testing (POCT) assays to rapidly and accurately identify SARS-CoV-2-infected patients. Additionally, asymptomatic and pre-asymptomatic SARS-CoV-2 infected patients are highly contagious and given the lack of appropriate detection assays, many SARS-CoV-2 infected patients have had contact with uninfected people before being identified for home isolation or hospitalisation (Du et al., 2020; Li et al., 2020a,b; F. Yu et al., 2020; P. Yu et al., 2020). Further, the SARS-CoV-2 outbreak coincided with seasonal

* Corresponding author.
** Corresponding author.
*** Corresponding author.
E-mail addresses: jitianxing7021@163.com (T. Ji), yangchaochen@cuhk.edu.hk (Y. Chen), qiangzhou70@163.com (Q. Zhou).
[1] These authors contributed equally to this work.

https://doi.org/10.1016/j.bios.2020.112455
Received 31 March 2020; Received in revised form 13 July 2020; Accepted 14 July 2020
Available online 21 July 2020

influenza (Bordi et al., 2020). The simultaneous visits of influenza patients to hospitals also contributed to the increasing spread of the SARS-CoV-2 infection due to the high nosocomial transmission of the virus (Wang et al., 2020). A fast, cheap, and highly-accurate POCT method is therefore urgently needed for timely isolation of infected cases and effective contact tracing of potential SARS-CoV-2 infected cases (Hellewell et al., 2020).

In this review, we first introduce the structure of the virus particle and the genome and gene expression characteristics of SARS-CoV-2. Then, the current SARS-CoV-2 RNA, virus particle, antigen, and antibody detection methods is summarised (Fig. 1). The problems related to false-positive and false-negative results in clinical practice and the unresolved challenges in this context are also discussed. Further, the paper outlines potentially promising novel detection approaches, including a novel nanoparticle-based lateral flow assay, electrochemical biosensors, and microfluidic chips, which may be employed to improve the performance of COVID-19 detection assays in the future. Finally, we discuss future research plans for the development of highly accurate, cheap, easy-use, point-of-care SARS-CoV-2 detection methods by utilising current portable detection technology.

2. Overview of SARS-CoV-2

SARS-CoV-2 belongs to the genus β-coronavirus which is comprised of crown-like, enveloped, positive-sense single-stranded RNA (+ssRNA) viruses (Fig. 2A). In coronavirus particles, the nucleocapsid protein (NP) packages the genome RNA to form a helical nucleocapsid (Masters, 2019). Membrane (M) proteins are located at the intracellular membrane structure and bind to internal nucleoproteins to form the core structure (Fig. 2A) (Escors et al., 2001). Further, the envelope (E) protein, the M protein, and the spike protein (SP) interact with each other to form a viral envelope, where the SP protrudes from the viral envelope by binding to the M protein (Fig. 2A) (Neuman et al., 2006; Rota et al., 2003; Schoeman and Fielding, 2019). Among the structural proteins, the SP facilitates viral entry into host cells by using its receptor-binding domain (RBD) region to bind to host cell receptors. As such, the severe acute respiratory syndrome coronavirus (SARS-CoV) and SARS-CoV-2 have been found to use the receptor angiotensin-converting enzyme 2 (ACE2) for entry into host cells (Hoffmann et al., 2020). The RBD region of the SP is, therefore, the major target for SARS-CoV-2 therapy and detection. An anti-SP antibody assay can be used to screen serum containing high titres of SARS-CoV-2 neutralising antibodies targeting the SP and this serum can be used to treat severe COVID-19 patients (Bloch et al., 2020; Okba et al., 2020). Additionally, the NP also exhibits high immunogenicity and anti-NP antibodies have been used to detect coronavirus infection (Bloch et al., 2020; Okba et al., 2020). The NP can also be secreted into body fluids upon early infection and has the potential to be used as a biomarker for antigen detection (Che et al., 2004).

The genome sequence length of SARS-CoV-2 is about 30 kb, with a 5′-cap structure and 3′-poly-(A) tail enveloped by a complex of structural proteins to form a crown-like, enveloped virus (Fig. 2A) (Chan et al., 2020a). Similar to other β-CoVs, the SARS-CoV-2 genome is arranged in the following order: 5′ cap structure-replicase (open reading frame1/ab, ORF1/ab)-structural proteins with a [spike(S)-E-M-nucleocapsid (N)]-3′poly (A) tail (Fig. 2A) (Chan et al., 2020a). Upon entry into cells, the genomic RNA (gRNA) is used as a template to directly translate polyprotein (pp) 1a/1ab which is processed into 16 non-structural proteins (Nsps) by proteolytic cleavage (Fig. 2B). The functions of these Nsps are shown in Fig. 2F (Chan et al., 2020a). Most Nsps assemble into replication and transcription complexes (RTCs) and are involved in the transcription and replication of the coronavirus (Perlman and Netland, 2009). The viral genome is also used as the template for generating negative-sense RNA intermediates which, subsequently, serve as templates for the synthesis of positive-sense gRNA and sub-genomic RNAs (sgRNAs) by RTCs, in a manner of discontinuous transcription (Fig. 2B) (Sawicki et al., 2007). Finally, the sgRNAs are translated into structural proteins and accessory proteins that are involved in coronavirus

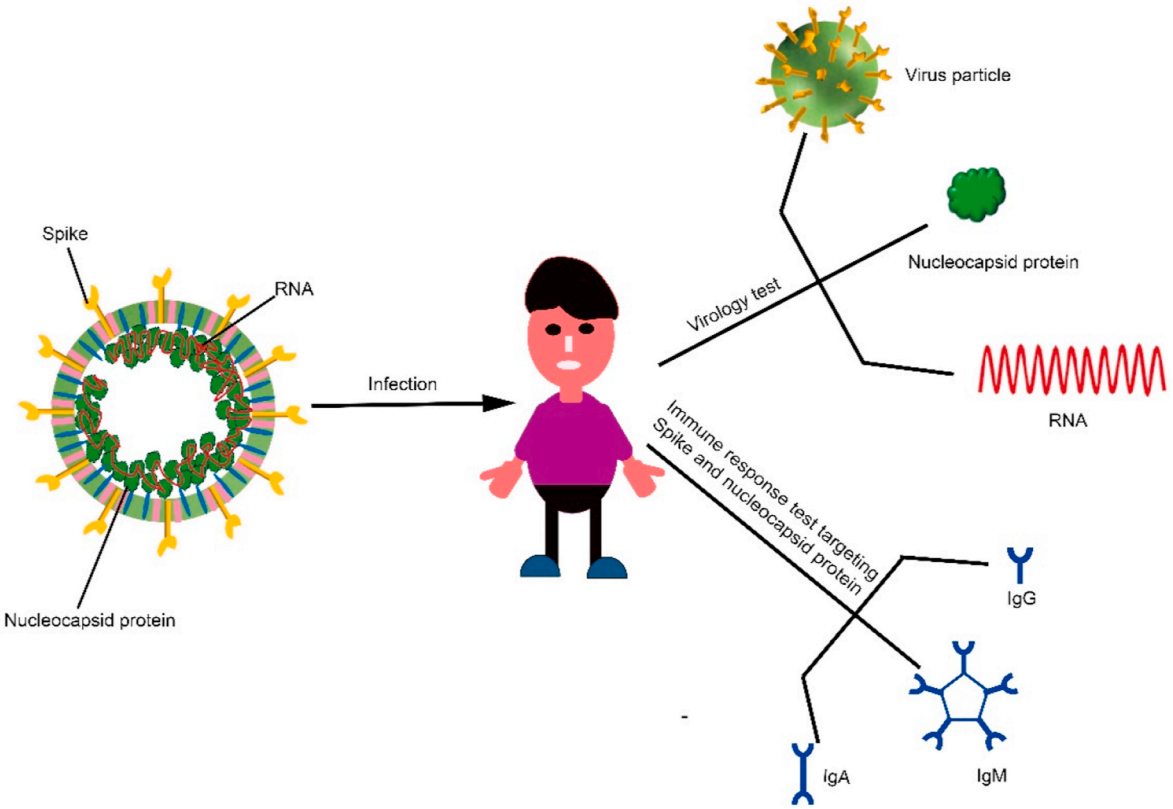

Fig. 1. Schematic illustration of strategies for the detection of COVID-19 patients.

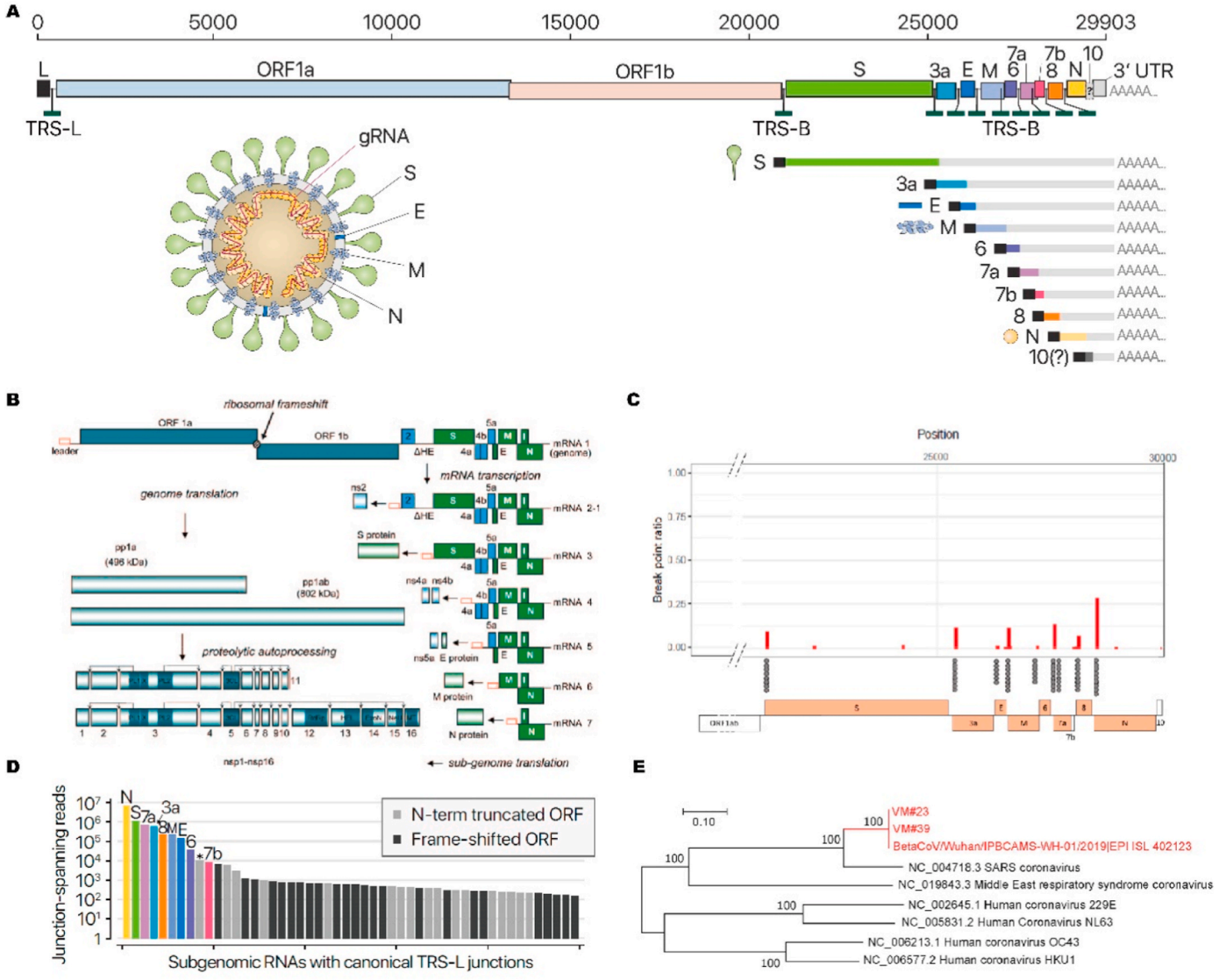

F

NSP	Putative function/domain	Amino acid position	Putative cleave site
nsp1	suppress antiviral host response	M1 – G180	(LNGG'AYTR)
nsp2	unknown	A181 – G818	(LKGG'APTK)
nsp3	putative PL-pro domain	A819 – G2763	(LKGG'KIVN)
nsp4	complex with nsp3 and 6: DMV formation	K2764 – Q3263	(AVLQ'SGFR)
nsp5	3CL-pro domain	S3264 – Q3569	(VTFQ'SAVK)
nsp6	complex with nsp3 and 4: DMV formation	S3570 – Q3859	(ATVQ'SKMS)
nsp7	complex with nsp8: primase	S3860 – Q3942	(ATLQ'AIAS)
nsp8	complex with nsp7: primase	A3943 – Q4140	(VKLQ'NNEL)
nsp9	RNA/DNA binding activity	N4141 – Q4253	(VRLQ'AGNA)
nsp10	complex with nsp14: replication fidelity	A4254 – Q4392	(PMLQ'SADA)
nsp11	short peptide at the end of orf1a	S4393 – V4405	(end of orf1a)
nsp12	RNA-dependent RNA polymerase	S4393 – Q5324	(TVLQ'AVGA)
nsp13	helicase	A5325 – Q5925	(ATLQ'AENV)
nsp14	ExoN: 3′–5′ exonuclease	A5926 – Q6452	(TRLQ'SLEN)
nsp15	XendoU: poly(U)-specific endoribonuclease	S6453 – Q6798	(PKLQ'SSQA)
nsp16	2′-O-MT: 2′-O-ribose methyltransferase	S6799 – N7096	(end of orf1b)

(caption on next page)

Fig. 2. Schematic illustration of the structure of the coronavirus genome and virion, the mechanism of coronavirus replication and transcription, and the expression abundance of sgRNA. (A) Schematic presentation of the SARS-CoV-2 genome organisation, the canonical subgenomic mRNA, and the virus structure. The black box indicates the leader sequence. Note that our data show no evidence for open reading frame 10 (ORF10) expression. S: spike protein, E: envelop protein, M: membrane protein, N: nucleocapsid protein, gRNA: genomic RNA, TRS-L: transcriptional regulatory sequences-leader, TRS-B: transcriptional regulatory sequences-body. Reproduced with permission from (Kim et al., 2020c). (B) Mechanism of coronavirus replication and transcription. The virus open reading frames (ORFs) are depicted in teal (nsp1-nsp16 genes), blue (ns2, ns4a, ns4b, and ns5a genes), and green (S, M, E, N, and I structural protein genes). The open red box represents the common 59-leader sequence and the barred circle represents the programmed (−1) frameshifting element. The translation products of the genome- and subgenome-length mRNAs are depicted, and the autoproteolytic processing of the ORF1a and ORF1a/ORF1b polyproteins into proteins nsp1 to nsp16 is shown. A number of confirmed and putative functional domains in the nsp proteins are also indicated. NeU, uridylate-specific endoribonuclease; PL1, papain-like protease 1; PL2, papain-like protease 2. Reproduced with permission from (Sawicki et al., 2007). (C) The relative abundance of sgRNA in vivo. Top, the break point ratios; middle, the TRS sequences within the SARS-COV-2 genome, solid dots indicate a matching base to the leader TRS sequence while a hollow one indicates a mismatch; bottom, schematic showing SARS-COV-2 annotation, the ORF supported by sgRNAs is indicated by the orange colour. Reproduced with permission from (Lv et al., 2020). (D) Top 50 expressed SARS-CoV-2 sgRNAs in Vero cells. The asterisk indicates an ORF beginning at 27,825, which may encode the 7b protein with an N-terminal truncation of 23 amino acids. The grey bars denote minor transcripts that encode proteins with an N-terminal truncation compared with the corresponding overlapping transcript. The black bars indicate minor transcripts that encode proteins in a different reading frame from the overlapping major mRNA. Reproduced with permission from (Kim et al., 2020c). (E) Phylogenetic tree of SARS-CoV-2 and other pathogenic human CoVs, including HCoV-229E, HCoV-HKU1, HCoV-NL63 HCoV-OC43, and MERS-CoV. Reproduced with permission from (Hou et al., 2020). (F) Putative function and proteolytic cleavage sites of 16 nonstructural protein in orf1a/b, as predicted by bioinformatics. Reproduced with permission from (Chan et al., 2020a). (For interpretation of the references to colour in this figure legend, the reader is referred to the Web version of this article.)

assembly (Fig. 2B) (Sawicki et al., 2007). Recently, the nanopore-based direct RNA sequencing approach has shown that N RNA is the most abundantly expressed transcript in SARS-CoV-2 infected cells, followed by S, 7a, 3a, 8, M, E, 6, and 7b. This suggests that the N gene is one of the best targets for high-sensitivity detection of SARS-CoV-2 infection (Fig. 2C and D) (Kim et al., 2020c). However, compared with SARS-CoV and the Middle East respiratory syndrome coronavirus (MERS-CoV), SARS-CoV-2 has lower NP expression and higher SP expression, and this may contribute to SARS-CoV-2 being more contagious than the former viruses (Lv et al., 2020). Thus, collectively, the SARS-CoV-2 virus particle, RNA, NP antigen, and human antibodies targeting the SP and the NP are used for accurately screening COVID-19 patients (Fig. 1).

Phylogenetic analysis, based on the complete genome, indicates that the SARS-CoV-2 clusters with bat-SARS like Cov and SARS-CoV rather than other human coronaviruses (HCoVs) such as HCoV-229E, HCoV-HKU1, HCoV-NL63 HCoV-OC43, and MERS-CoV (Fig. 2E) (Hou et al., 2020). Many of the clinical symptoms of SARS-CoV-2 infection are very similar to SARS-CoV and influenza infections (L. Pan et al., 2020; Y. Pan et al., 2020). The fatality rate of SARS-CoV infection is 3.2%, significantly lower than that of SARS-CoV-2 infection (10%) (Liang et al., 2020). SARS-CoV-2 is, however, more contagious than SARS-CoV and this may be related to the higher viral load of SARS-CoV-2 in the upper respiratory tract of pre-symptomatic and asymptomatic SARS-CoV-2 infected patients (Kimball et al., 2020; Wei et al., 2020). This poses a significant challenge for controlling the spread of the COVID-19 virus.

3. Nucleotide detection assay

During the early period of the SARS-CoV-2 outbreak, many SARS-CoV-2 infected patients were identified in a timely manner due to the rapid development and widespread use of deoxyribonucleic acid (DNA) sequencing technology and the reverse transcription-polymerase chain reaction (RT-PCR) method (Zhou et al., 2020). DNA sequencing technology can be used to explore novel mutations and the evolution of SARS-CoV-2 isolates (Shen et al., 2020). DNA sequencing assays, however, require highly professional technicians to operate expensive instruments under stringent laboratory conditions. These methods are time-consuming and relatively expensive, which thereby significantly limit their extensive application for identifying SARS-CoV-2 infections (Ai et al., 2020). Compared to sequencing technology, the RT-PCR detection method is cheaper, easier and widely used, and has a short turn-around time (Ai et al., 2020). Therefore, many institutes and companies have developed SARS-CoV-2 RT-PCR detection methods which have played key roles in controlling the SARS-CoV-2 further spreading (Ai et al., 2020).

3.1. Commercial nucleotide detection methods

Many molecular diagnostic companies and institutes are striving to develop an integrated, random-access, point-of-care molecular devices for faster and more accurate diagnosis of SARS-CoV-2 infection (Loeffelholz and Tang, 2020). As of April 19, 2020, the Food and Drug Administration (FDA) has approved more than 37 SARS-CoV-2 RNA detection kits (Supplemental Table 1) (https://www.fda.gov/medical-devices/emergency-use-authorizations-medical-devices/coronavirus-disease-2019-covid-19-emergency-use-authorizations-medical-devices). The majority of the approved molecular detection kits uses multiplex RT-PCR to detect more than two target regions in order to enhance the detection sensitivity of the kit. In this process, two or more target RNA regions are, first, simultaneously transcribed into complementary DNA (cDNA) by reverse transcriptase and, then, these cDNAs are used as the template for extension. During the extension phase, the 5'→3′ exonuclease activity of the Taq polymerase cleaves the annealed probe, releasing the reporter dye from the 3′ quenching dye, resulting in an increase of fluorescence signal proportional to the amount of amplified product (Supplemental Table 1). Seven companies have developed enclosed detection cartridges that combine RNA extraction, purification, amplification and detection to reduce cross-contamination, and the number of steps that require human operation. This significantly increases the detection repeatability and reduces technician infection risk. DiaSorin Molecular LLC developed an RT-PCR detection assay that enables the direct amplification of SARS-CoV-2 RNA from clinical samples without RNA extraction (Supplemental Table 1). Two companies have adopted isothermal multiplex nucleic acid amplification for field-deploy detection of SARS-CoV-2. For example, ID NOW COVID-19 has a detection sensitivity of 125 GE/mL, which is lower than many RT-PCR detection kits. More interestingly, ID NOW COVID-19 can deliver positive results in as little as 5 min and negative results in 13 min (Supplemental Table 1). The principle of ID NOW COVID-19 is the use of a nicking endonuclease isothermal amplification reaction to rapidly generate short amplicons, where detection is accomplished in real-time using fluorescently-labelled molecular beacons (Nie et al., 2014). Clinical comparative analysis has demonstrated, however, that 6% (6/96) of SARS-CoV-2 positive samples cannot be detected using ID NOW COVID-19 (Rhoads et al., 2020). Gnomegen developed a reverse transcription digital polymerase chain reaction (RT-dPCR) SARS-CoV-2 RNA detection kit which has the advantage of absolute quantification and is more sensitive for virus detection, compared to the RT-PCR kit (Supplemental Table 1.). The RT-dPCR kit is therefore a better choice for detecting low-viral-load samples and this approach could significantly increase COVID-19 screening capacity (F. Yu et al., 2020; P. Yu et al., 2020).

3.2. Non-commercialised RNA detection methods

Many institutes are keen to adopt isothermal nucleic acid amplification technology for the POCT of SARS-CoV-2, avoiding the need for a highly expensive thermal cycler. Loop-mediated isothermal amplification (LAMP) may be the most promising alternative to PCR since it offers several advantages in terms of specificity, sensitivity, reaction efficiency, and product yield (Table 1). In principle, LAMP relies on autocycling strand displacement DNA synthesis in the presence of Bst DNA polymerase, under isothermal conditions of 60 °C–65 °C. The reaction results in 10^6 to 10^9 copies of target DNA within 30–60 min. For example, Park et al. (2020) developed a reverse transcription (RT)-LAMP assay targeting Nsp3 for SARS-CoV-2 detection, of which the limit of detection (LOD) was 100 copies per reaction. Yan et al. (2020) prepared an RT-LAMP assay targeting ORF1ab and the S gene, of which the LOD was 20 copies/reaction and 200 copies/reaction, within 60 min. Moreover, the evaluation of a small clinical sample demonstrated that some of the developed RT-LAMP assays have a specificity of 100% and sensitivity of 100% (Table 1). In addition, crude cell lysate containing SARS-CoV-2 RNA can be effectively detected using the RT-LAMP method, avoiding the need for an RNA purification step (Zhang et al., 2020). Further, visual detection methods can be performed using dyes that utilise inherent by-products of extensive DNA synthesis such as malachite green, calcein, and hydroxynaphthol blue. Interestingly, Broughton et al. (2020) utilised a clustered regularly interspaced short palindromic repeat (CRISPR)-Cas12 lateral flow assay to enhance detection sensitivity, simplify the result read, and reduce the detection time of the RT-LAMP detection assay.

Research has also been devoted to utilising the collateral cleavage activity of Cas nucleases (e.g., Cas12a, Cas12b, and Cas13a) to develop point-of-care SARS-CoV-2 RNA detection assays (Fig. 3). For example, Hou et al. (2020) utilised polymerase-mediated DNA amplification by recombinase polymerase amplification (RPA) and CRISPR-Cas13-mediated enzymatic signal amplification for high sensitivity detection of SARS-CoV-2, with detection of 7.5 copies/reaction within 40 min (Fig. 3A). A clinical comparative analysis reported that the CRISPR-Cas13-based assay has a higher detection capacity than the RT-PCR assay (Hou et al., 2020). Similarly, Rauch et al. (2020) devised a method called CREST (Cas13-based, Rugged, Equitable, Scalable Testing) which takes advantage of widely available enzymes (i.e. Taq polymerase), low-cost thermocyclers, a linear amplification step (transcription), and CRISPR-Cas13-based fluorescence signal amplification to detect up to 10 copies/μL SARS-CoV-2 RNA. Lucia et al. (2020) developed an RPA-CRISPR-Cas12-based SARS-CoV-2 RNA detection assay with a LOD of 10 copies/μL. To further reduce complexity in the detection process, Ding et al. (2020) developed an All-In-One Dual CRISPR-Cas12a (AIOD-CRISPR) assay in which all components are incubated in a single reaction system to rapidly detect RNA with high sensitivity and specificity without separate pre-amplification steps. After optimisation of detection conditions, the LOD of the AIOD-CRISPR SARS-CoV-2 RNA detection assay was 4.6 copies of SARS-CoV-2 N RNA targets in 40 min.

In addition, Qiu et al. (2020) prepared a plasmonic chip with two-dimensional gold nanoislands which is capable of generating local plasmonic photothermal (PPT) heat and can simultaneously perform in situ hybridisation. The localised PPT heat can increase the in-situ hybridisation temperature and facilitate the accurate discrimination of two similar gene sequences to increase detection selectivity. This localised surface plasmon resonance (LSPR) sensing exhibits high sensitivity toward selected SARS-CoV-2 sequences, with a LOD of 0.22 pM. However, the high cost of the SPR detection instrument restricts its point-of-care application (Masson, 2017).

3.3. Factors that influence the detection performance of SARS-CoV-2 RT-PCR detection assays

Initially, the RT-PCR method mainly targeted the conservation region and the specific region of SARS-CoV-2 (Ai et al., 2020). RT-PCR methods targeting different regions, however, have different detection sensitivities. For example, Chu et al. (2020) developed one-step, quantitative, real-time, reverse-transcription PCR assays to detect the open reading frame 1b (ORF1b) and the N genes and subsequently demonstrated that the N gene assay was about 10 times more sensitive than the ORF1b gene assay in detecting positive clinical specimens. Corman et al. (2020) developed a one-step RT-PCR kit for the detection of RNA-dependent RNA polymerase (RdRP) and E and N genes. The RdRp gene assay demonstrated the highest sensitivity (Corman et al., 2020). In the meantime, the CDC announced primer and probe sets for the detection of different fragments of the N gene (N1, N2, N3) of SARS-CoV-2 (https://www.cdc.gov/coronavirus/SARS-CoV-2/lab/rt-pcr-panel-primer-probes.html). Recent clinical evaluations have further demonstrated that the N1, N2, and E gene detection assays have better detection performance than the RdRP and N3 detection assays (Nalla et al., 2020). More recently, Chan et al. (2020b) designed novel primers and probes for real-time RT-PCR detection of RdRp/Helicase (Hel) and S and N genes. These assays showed a higher detection sensitivity than the previously developed RdRp-P2 gene assay. Apparently, the RdRp/Hel detection assay exhibited higher detection sensitivity than other gene detection assays (Chan et al., 2020b). Comparative analysis of the detection of 273 specimens of 15 COVID-19 patients demonstrated a 43.6% positive rate for the RdRp/Hel detection assay, which was significantly higher than the RdRp-P2 gene assay

Table 1
The reported SARS-CoV-2 RNA RT-LAMP assay.

Target genes	Detection methods	Sample	LOD	Detection time	Clinical evaluation	Reference
ORF1a/b, S and N	Fluorescence or Colourimetric assay	Viral RNA	20 copies/reaction	30-min	Sensitivity:100% Specificity:100%	Huang et al.. (2020)
N, S and RdRp	Fluorescence or Colourimetric assay	Viral RNA	118.6 copies/reaction	20 min	Sensitivity:94% Specificity:90%	Lu et al. (2020a)
N	Colourimetric assay	Viral RNA	100 copies/reaction	30 min	Sensitivity:100% Specificity:98.70%	Baek et al. (2020)
ORF1a/b	Turbidity monitoring or Colourimetric assay	viral RNA	20 copies/reaction	60 min	Sensitivity:100% Specificity:100%	Yan et al. (2020)
Nsp3	Colourimetric assay	Viral RNA	100 copies/reaction	30 min	Not performed	Park et al. (2020)
RdRp	Colourimetric assay	Viral RNA	30 copies/reaction	40 min	Sensitivity:100% Specificity: not performed	Lu et al. (2020b)
ORF1a, N	Colourimetric assay	Viral RNA/crude cell lysate	120 copies/reaction(RNA) 80 copies/reaction (crude cell lysate)	30 min	Not performed	Zhang et al. (2020)

RdRp: RNA-dependent RNA polymerase.

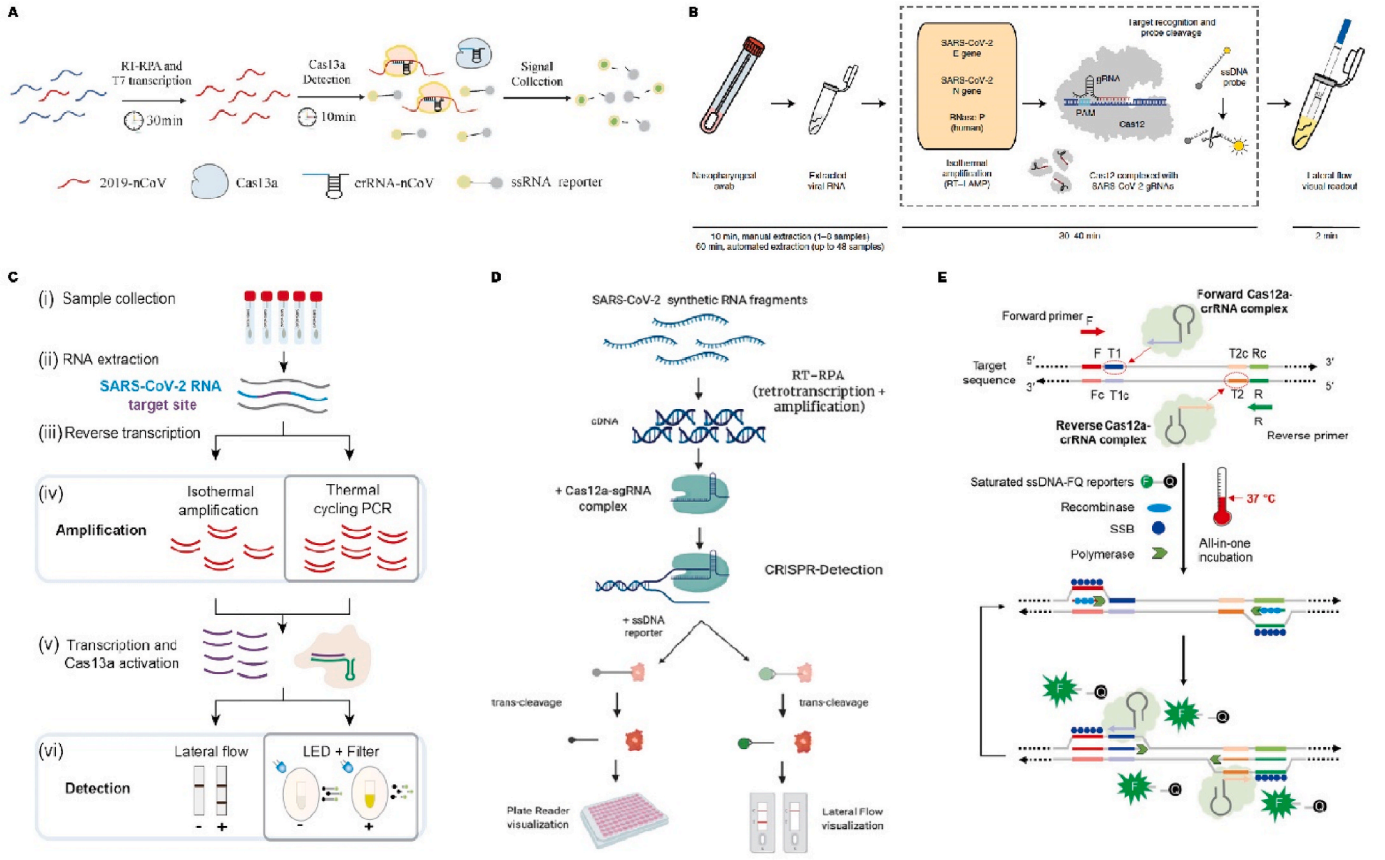

Fig. 3. Schematic illustration of CRISPR-based SARS-CoV-2 RNA detection assay. (A) CRISPR-Cas 13-nCoV test combining a recombinase polymerase amplification step with T7 transcription and Cas13 detection. Reproduced with permission from (Hou et al., 2020). (B) SARS-CoV-2 DETECTR workflow. Conventional RNA extraction was used as the input for DETECTR (LAMP preamplification and Cas12-based detection), followed by a fluorescent reader or lateral flow strip. Reproduced with permission from (Broughton et al., 2020). (C) Cas13-based, Rugged, Equitable, Scalable Testing (CREST) method. (i-iii) Standard sample collection, RNA extraction, and reverse transcription. (iv) Amplification using cost-effective Taq polymerase and portable thermocyclers instead of isothermal reactions. (v) Transcription and Cas13 activation are followed by visualisation with a blue LED (~495 nm) and orange filter. Reproduced with permission from (Rauch et al., 2020). (D) CRISPR-Cas 12-nCoV test coupling recombinase polymerase amplification with Cas12 collateral cleavage fluorescence detection or lateral flow strip detection. Reproduced with permission from (Lucia et al., 2020). (E) All-In-One Dual CRISPR-Cas12a assay. SSB, single-stranded DNA binding protein. Reproduced with permission from (Ding et al., 2020). (For interpretation of the references to colour in this figure legend, the reader is referred to the Web version of this article.)

(28.2%). Additionally, the RdRp/Hel detection assay was reported to be more sensitive than the RdRp-P2 assay for the detection of SARS-CoV-2 RNA in nasopharyngeal aspirate/swabs, throat swabs, saliva, and plasma (Chan et al., 2020b). More importantly, the RdRp/Hel detection assay had no cross-reaction with SARS-CoV cell culture lysate. The RdRp-P2 assay, however, had a positive signal in SARS-CoV cell culture lysate, but not in SARS-CoV cell culture supernatants (Chan et al., 2020b; Corman et al., 2020), which implies that the RdRp-P2 assay has a degree of cross-reaction with SARS-CoV. Recently, Yip et al. (2020) utilised their in-house program, GolayMetaMiner, to deduce a novel molecular detection target, Nsp2, which is SARS-CoV-2 specific and highly conserved among globally-detected SARS-CoV-2 isolates. Then, the researchers developed an Nsp2 RT-PCR detection assay that has similar detection sensitivity and clinical sample detection performance to the RdRp/Hel detection assay (Yip et al., 2020). The common target genes, related primers, and probe sets are summarised in Table 2.

Additionally, the positive rate of RT-PCR RNA detection has been shown to be dependent on the sample type, with differences between bronchoalveolar lavage fluid (93%), fibrobronchoscope brush biopsy (46%), sputum (72%), nasal swabs (63%), pharyngeal swabs (32%), faeces (29%), and blood (1%) (Wang et al., 2020). Interestingly, the use of saliva for SARS-CoV-2 detection has been found to be more sensitive and reliable than the use of nasopharyngeal swabs (NS). Saliva sampling is an appealing alternative for high sensitivity COVID-19 detection since saliva collection is non-invasive and easy to self-perform (Azzi et al., 2020; Wyllie et al., 2020). Moreover, a study by Lippi et al. suggested that pre-analytical errors, specimen collection errors, and transportation factors also have an impact on assay detection accuracy (Lippi et al., 2020). Further, the positive rate declines with the recovery of the COVID-19 patients due to the gradual decrease in viral load (Fig. 4) (Zhao et al., 2020), therefore, a high fraction of COVID-19 patients with a low virus load cannot be identified promptly with the RT-PCR method (Xie et al., 2020a,b).

4. SARS-CoV-2 virus particle detection

Another COVID-19 detection method involves the direct detection of SARS-CoV-2 virus particles using immunoassays. For instance, Seo et al. (2020) utilised an anti-spike antibody which can bind to SARS-CoV-2 virus particles to fabricate graphene-based field-effect-transistor (FET) biosensors (Fig. 5). These FET biosensors can respond to 16 pfu/mL of virus particles in PBS within 10 min. However, it was found that the solution commonly used to store respiratory virus samples, the universal transport medium (UTM), can produce a high noise signal and thus, the LOD in UTM decreased to 242 copies/mL (Seo et al., 2020). Novel materials or engineering methods must be developed to reduce noise signals in FET biosensors, and thereby improving the signal-to-noise ratio to allow high sensitivity screening of low virus load COVID-19 patients

Table 2
Commonly used target genes and related primer and probe sets for RT-PCR SARS-CoV-2 detection.

Ref.	Target genes	Detection methods	Forward	Reverse	Probe
Yip et al. (2020)	NSP2	SYBR Green RT-PCR	ATGCATTTGCATCAGAGGCT	TTGTTATAGCGGCCTTCTGT	
Chan et al. (2020b)	RdRp/ Helicase	TaqMan RT-PCR	CGCATACAGTCTTRCAGGCT	GTGTGATGTTGAWATGACATGGTC	FAM-TTAAGATGTGGTGCTTGCATACGTAGAC-lABkFQ
	Spike	TaqMan RT-PCR	CCTACTAAATTAAATGATCTCTGCTTTACT	CAAGCTATAACGCAGCCTGTA	HEX-CGCTCCAGGGCAAACTGGAAAG-IABkFQ
	Nucleocapsid	TaqMan RT-PCR	GCGTTCTTCGGAATGTCG	TTGGATCTTTGTCATCCAATTTG	FAM-AACGTGGTTGACCTACACAGST-lABkFQ
CDC[a]	Nucleocapsid (N1)	TaqMan RT-PCR	GACCCCAAAATCAGCGAAAT	TCTGGTTACTGCCAG TTGAATCTG	FAM-ACCCCGCATTACGTTTGGTGG ACC-BHQ1
	Nucleocapsid (N2)	TaqMan RT-PCR	TTACAAACATTGGCCGCAAA	GCGCGAATTCCGAA GAA	FAM-ACAATTTGCCCCCAG CGCTTCAG-BHQ1
	Nucleocapsid (N3)	TaqMan RT-PCR	GGGAGCCTTGAATACACCAAAA	TGTAGCACGATT GCAGCATTG	FAM-AYCACATTGGCA CCCGCAATCCTG-BHQ1
Corman et al. (2020)	RdRP gene	TaqMan RT-PCR	GTGARATGGTCATGTGTGGCGG	CARATGTTAAASACACTATTAGCATA	P1:FAM-CCAGGTGGWACRTCATCMGGTGATGC-BBQ P2: FAM-CAGGTGGAACCTCATCAGGAGATGC-BBQ
	Envelop	TaqMan RT-PCR	ACAGGTACGTTAATAGTTAATAGCGT	ATATTGCAGCAGTACGCACACA	FAM-ACACTAGCCATCCTTACTGCGCTTCG-BBQ
	Nucleocapsid	TaqMan RT-PCR	CACATTGGCACCCGCAATC	GAGGAACGAGAAGAGGCTTG	FAM-ACTTCCTCAAGGAACAACATTGCCA-BBQ
Chu et al. (2020)	ORF1b	TaqMan RT-PCR	TGGGGYTTTACRGGTAACCT	AACRCGCTTAACAAAGCACTC	FAM-TAGTTGTGATGCWADTCATGACTAG-IBFQ
	Nucleocapsid	TaqMan RT-PCR	TAATCAGACAAGGAACTGATTA	CGAAGGTGTGACTTCCATG	FAM-GCAAATTGTGCAATTTGCGG-IBFQ

[a] Division of Viral Diseases. 2020. 2019-Novel Coronavirus (SARS-CoV-2) Real-time rRT-PCR Panel Primers and Probes. Centers for Disease Control and Prevention. https://www.cdc.gov/coronavirus/SARS-CoV-2/lab/rt-pcr-panel-primer-probes.html.

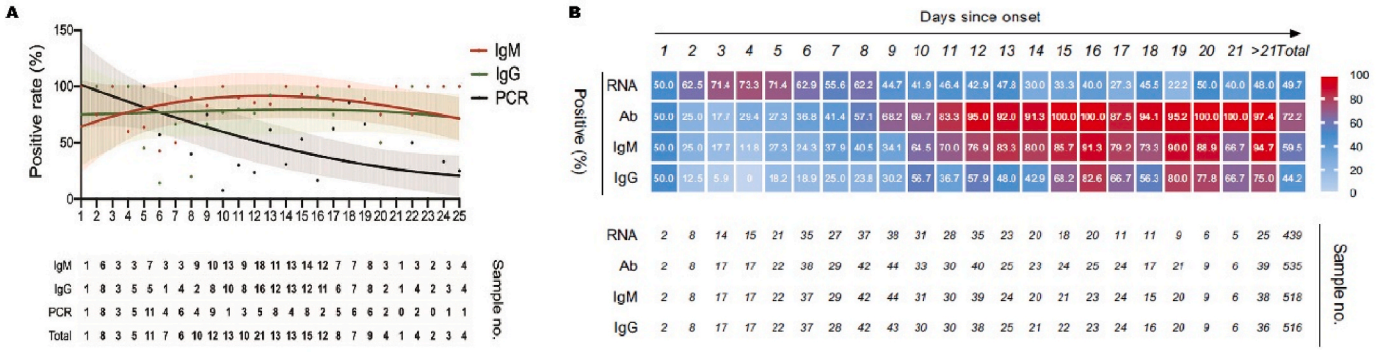

Fig. 4. Fitted curve of the COVID-19 detection positive rate, by PCR, IgM, and IgG enzyme-linked immunosorbent assay (ELISA), on different days after symptom onset. (A) SARS-CoV-2 RNA and antibodies IgG and IgM targeting the NP. Reproduced with permission from (Guo et al., 2020a,b). (A) SARS-CoV-2 RNA and total antibodies IgG and IgM targeting receptor bind region (RBD) of SP. Reproduced with permission from (Zhao et al., 2020).

(Hwang et al., 2020). Moreover, coupling FET sensors with magnetic particle pre-concentration before detection can minimise the effect of interferents on sample matrix by attracting immunocomplex onto the surface of the sensor via an external magnetic field, thereby increasing detection sensitivity and producing a high signal-noise ratio (Farka et al., 2017).

5. NP antigen detection assay

Previous studies have shown that the coronavirus NP is the predominant, virus-derived, structural protein released in large amounts into the serum, nasopharyngeal aspirate, throat wash samples, faecal material, and urine during the early period of infection (Das et al., 2010). Detection of the NP antigen might therefore be an effective strategy for the early screening of suspected SARS-CoV or MERS-CoV-infected patients (Woo et al., 2018). Accordingly, Mass spectrometric analysis has demonstrated that NP is present in gargle solution samples from COVID-19 patients, suggesting that coronavirus SARS-CoV-2 NP antigen POCT could be effective for the early identification of COVID-19 patients (Ihling et al., 2020). Just recently, antibody pairs for SARS-CoV-2 NP detection were prepared using high-specificity peptide-immunised Balb/c mice and New Zealand White rabbits (Li et al., 2020). Subsequently, an ELISA and quantum dot-based lateral flow assay were developed for the detection of SARS-CoV-2 NP with a LOD of 100 ng/mL and 10 ng/mL, respectively (Li et al., 2020). Additionally, Diao et al. (2020) developed a SARS-CoV-2 NP fluorescence lateral flow assay which demonstrated a sensitivity of 68% and a specificity of 100% in NS samples. In addition, SARS-CoV-2 NP may be detected in NS specimens of COVID-19 patients within three days of onset of fever (Diao et al., 2020). More interestingly, the NP antigen was detected in the urine of 73.6% (14/19) of patients diagnosed with COVID-19 (Diao et al., 2020). Previous research reported that SARS-CoV

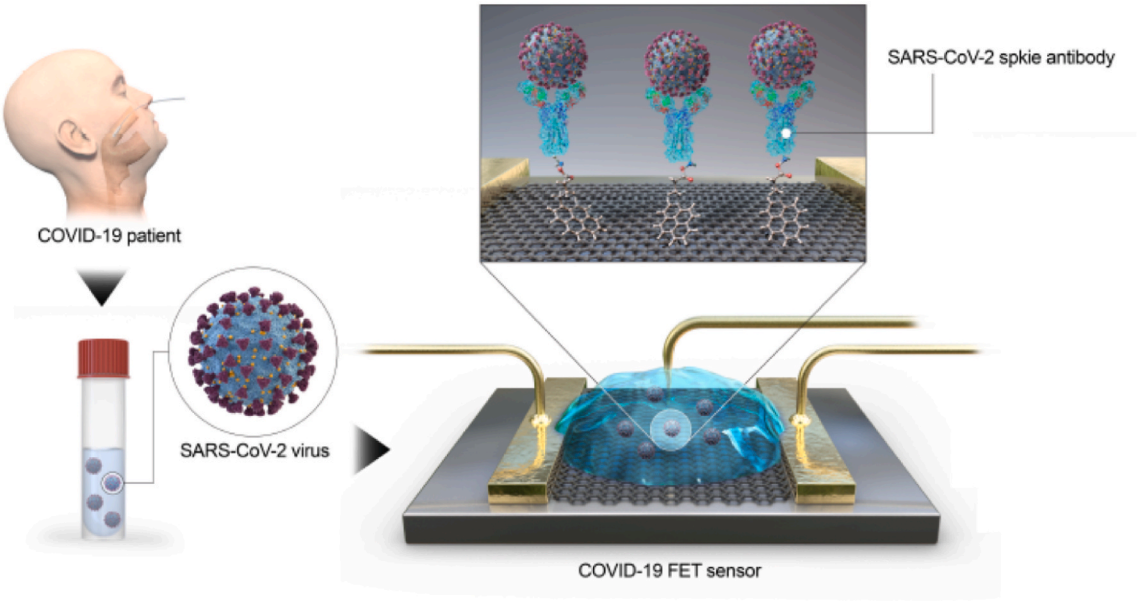

Fig. 5. Schematic diagram of COVID-19 FET sensor operation procedure. Graphene as sensing material is selected and SARS-CoV-2 spike antibody is conjugated onto the graphene sheet via 1-pyrenebutyric acid n hydroxysuccinimide ester, which is an interfacing molecule used as a probe linker. Reproduced with permission from (Seo et al., 2020).

NP was only detected in the urine of 8% of SARS patients (Lau et al., 2005). The apparent high SARS-CoV-2 NP positive rate in urine of COVID-19 patients must be verified by testing a larger number of clinical samples. It should be noted that NP expression was lower in SARS-CoV-2 than in SARS-CoV and MERS-CoV, suggesting that the concentration of N protein in bodily fluid in SARS-CoV-2 patients could be low (Lv et al., 2020). Highly sensitive detection technologies are therefore urgently needed to achieve point-of-care antigen detection.

6. Antibody detection assays

6.1. Antibody detection assays targeting SP

Body fluid antibody detection is another effective strategy for the identification of coronavirus infection. To date, two blood antibody assays have been developed for quick SARS-CoV-2 detection. The first method detects the serum antibody, IgG/IgM, targeting the RBD of the SP of SARS-CoV-2. This assay has a specificity of 90.63% and a sensitivity of 88.66% (Li et al., 2020). However, the amine acid sequences of the RBD of SARS-CoV-2 share 72% similarity with that of SARS-CoV (Chan et al., 2020a); thus, some antibodies targeting the RBD of SARS-CoV could bind to the RBD of SARS-CoV-2 (Tian et al., 2020). False-positive anti-RBD antibody results may be observed in previously infected SARS-CoV patients (Guo et al., 2020a,b). Cai et al. (2020) found that one peptide from the S-based antibody IgM assay had a high specificity, of 100%, but a lower sensitivity of 71.4%. In addition, total antibody detection with RBD double-antigen sandwich methodology is reported to have higher sensitivity than anti-RBD IgM or IgG, especially in the early period of COVID-19 infection (Lou et al., 2020).

6.2. Antibody detection assays targeting NP

With regard to anti-NP antibody, Guo et al. (2020a,b) reported that the positive rates of anti-NP-IgM and anti-NP-IgA in 208 plasma samples from COVID-2019 patients were 90.4% and 93.3%, respectively, higher than those of anti-NP-IgG (77.9%). Interestingly, the positive rate of anti-NP-IgA in the early period (1–7 days) reached 92.7%, which was higher than anti-NP-IgM (85.4%) (Guo et al., 2020a,b). Consistent with the RBD double-antigen detection method, the NP double-antigen detection method can also facilitate the early identification of COVID-19 patients. Importantly, a high positive rate (93.1%; 54/58) of anti-NP-IgM antibodies was reported in patients with positive clinical manifestations, abnormal chest radiography imaging findings, and contact history with COVID-19 patients However, the virus was not detected in these patients using deep sequencing or qPCR assay. This indicates that anti-NP-IgM detection combined with RT-PCR detection could significantly enhance the diagnosis of COVID-19 infections with negative RT-PCR results (Guo et al., 2020a,b).

6.3. Antibody detection assays combinational targeting NP and SP

More interestingly, some COVID-19 patients have earlier seropositivity for anti-RBD than for anti-NP, for both IgG and IgM (Liu et al., 2020a,b; To et al., 2020); in contrast to SARS patients who have higher anti-NP antibodies than anti-SP antibodies (Woo et al., 2005). Unexpectedly, the earlier seroconversions of COVID-19 patients for anti-NP and anti-RBD IgG were higher than those for anti-NP and anti-RBD IgM, and the total positive rate of anti-RBD IgG/IgM was higher than anti-NP IgG/IgM (To et al., 2020). Moreover, some COVID-19 patients have single anti-SP or anti-NP antibody seroconversion (Liu et al., 2020a,b). Combining anti-NP with anti-RBD antibody detection is therefore a more effective strategy for achieving increased screening capacity for COVID-19. Accordingly, some companies have developed an anti-SP/NP-based antibody IgG/IgM chemiluminescence detection kit which has a specificity and sensitivity of 90% and 95% for IgG, and 80% and 95% for IgG (Qu et al., 2020). More importantly, the combination of anti-NP and anti-SP antibody detection could significantly increase the positive rate from 41.7% to 75% within one week after symptom onset (Sun et al., 2020).

6.4. The factors that influence antibody detection performance

The seroconversion of the anti-RBD antibody occurs 11–14 days after the onset of morbidity (Zhao et al., 2020). The seroconversion of anti-NP IgM, in some patients, occurs 7–12 days after the onset of morbidity (Zhang et al., 2020) and, in some patients, one day after symptom onset (Guo et al., 2020a,b); suggesting that seroconversion times vary between people. Moreover, some COVID-19 patients only have single

anti-SP or anti-NP antibody seroconversion, implying that there are different immune responses to NP and RBD among people. The sample collection time during the illness process and host immune factors could therefore contribute to false-negative results (Guo et al., 2020a,b). Moreover, the amino acid sequences of the RBD and NP of SARS-CoV-2 share significant similarities to that of SARS-CoV (Chan et al., 2020a; Guo et al., 2020a,b). Thus, false-positive antibody results may be observed in previously infected SARS-CoV patients (Guo et al., 2020a,b; Tian et al., 2020).

7. The unmet problem for SARS-CoV-2 detection

7.1. The unmet problems for SARS-CoV-2 RNA detection

There has been significant progress in SARS-CoV-2 molecular detection assays and this has significantly contributed to obtaining control of the COVID-19 pandemic. However, the low detection sensitivity of SARS-CoV-2 RNA POCT detection, especially using samples without RNA extraction, hinders the screening accuracy of pre-symptomatic and asymptomatic patients with low viral loads (L. Pan et al., 2020; Y. Pan et al., 2020). Further, longer times are needed for the detection of SARS-CoV-2, and this is not conducive to rapid and in-field screening of suspected COVID-19 patients. There is therefore an urgent need for the development of a rapid and simple method for the highly effective release and enrichment of SARS-CoV-2 RNA, which can be directly used for detection (He et al., 2017; Nyan et al., 2014). The ideal strategy could be the integration of RNA release through pre-concentration as well as amplification and detection in portable microfluidic-based cartridges or chips, which could enable point-of-care SARS-CoV-2 testing outside of the clinical diagnostic laboratory; in places such as airports, local emergency departments, and clinics (Dincer et al., 2019; Jin et al., 2018; Ouyang and Han, 2020).

7.2. The unmet problems for SARS-CoV-2 NP antigen and virus particle detection

In real clinical settings, low virus loads have been frequently observed in some COVID-19 patients (L. Pan et al., 2020; Y. Pan et al., 2020). There is a lack of an ultrasensitive SARS-CoV-2 virus particle detection method that could accurately identify COVID-19 patients. In addition, NP expression was lower in SARS-CoV-2 infected cells than in SARS-CoV and MERS-CoV infected cells, suggesting that the concentration of NP in the body fluid of SARS-CoV-2 patients is low (Lv et al., 2020). Highly sensitive detection technologies are therefore urgently needed to achieve point-of-care antigen or virus particle detection. Finally, the contents of SARS-CoV-2 NP in different sample types from COVID-19 patients, taken at different times during the illness, must be clarified to verify the early diagnostic and prognostic potential of SARS-CoV-2 NP detection.

7.3. The unmet problems for SARS-CoV-2 antibodies detection

As mentioned earlier, some coronavirus-infected patients have no seroconversion and have a low anti-SP antibody level; thus, a more sensitive detection method to accurately identify these infected patients is urgently needed (Okba et al., 2019). Additionally, the levels of anti-RBD and anti-NP antibodies are very low in the early phases of the illness process; thence a low observed positive rate in these stages (Fig. 4). The FDA and National Medical Products Administration (NMPA) have approved the anti-SARS-CoV-2 antibody colloidal gold lateral flow assay (CGLFA) and it is the most commonly used POCT kit due to its ease of use, low cost, and suitability for mass production (Table 3). COVID-19 patients with only trace levels of the target SARS-CoV-2 antibody are very likely to be neglected by the commercial CGLFA which has low sensitivity. Additionally, the incubation time of COVID-2019 is 5–6 days (Backer et al., 2020; Lauer et al., 2020). Thus, it is very possible that pre-asymptomatic and asymptomatic patients can spread the virus to their close contacts before these patients can be identified using anti-RBD and anti-NP antibody assays (L. Pan et al., 2020; Y. Pan et al., 2020). There is an urgent need for the development of a smarter, cheaper, and easier-to-use detection method that is more sensitive for the detection of targeted SARS-CoV-2 antibodies.

8. Potential biosensors for point-of-care SARS-CoV-2 detection

8.1. Lateral flow assay (LFA)

The LFA is user-friendly, cheap, and easily mass-produced. Many commercial colloidal gold anti-SARS-CoV-2 antibody LFAs have been used globally in an attempt to control the COVID-19 pandemic. In addition, LFAs may be the optimal method for in-field detection of SARS-CoV-2 antigens and RNA. The detection sensitivity of the LFA is, however, too low to achieve highly accurate screening of COVID-19 patients. Encouragingly, the detection sensitivity of the LFA has been improved with the use of novel nanomaterials as immunolabels such as quantum dots, up-conversion nanoparticles, and magnetic nanoparticles (Huang et al., 2016). Among them, LFAs that use ultra-bright fluorescence nanomaterials with longer fluorescence lifetimes can significantly reduce background noise and enhance LFA detection sensitivity using the time-resolved analysis technique (C. Hu et al., 2017; L. M. Hu et al., 2017). Additionally, a recent study reported a very promising near-infrared (NIR) wavelength emitting lanthanide-doped nanoparticles (UCNP)-based LFA which exhibits no fluorescence absorbance or auto-fluorescence interference with blood, stools, and nitrocellulose membranes, and can detect disease biomarkers with high accuracy and sensitivity (Kim et al., 2018; Liu et al., 2020a,b). Compared to fluorescence LFA detection, magnetic nanoparticle-based detection produces a much lower background magnetic signal, has a higher signal-noise ratio, and can detect disease biomarkers with higher sensitivity. Magnetic nanoparticle LFA detection is accomplished by measuring magnetic flux using a small magnetic assay reader under a magnetic field, or by measuring magnetisation saturation using small giant magnetoresistance-based sensors under an oscillating magnetic field (Huang et al., 2016). The use of the above LFAs, together with microfluidics or nucleic acid isothermal exponential amplification, hold considerable promise for rapid in-field detection of SARS-CoV-2 RNA with high sensitivity (Phillips et al., 2018; Reboud et al., 2019).

8.2. Electrochemical biosensors

Another very promising type of biosensor for highly sensitive point-of-care SARS-CoV-2 detection is the electrochemical biosensor. Electrochemical biosensors have been widely used to detect nucleic acids, proteins, small molecular antibodies, and viruses. They are simple and cost-effective smart sensing systems for rapid, high-sensitivity detection (Dai and Liu, 2019). In electrochemical sensors (EISs), the target is recognised using an antigen-antibody reaction, DNA, RNA, or peptide nucleic acid (PNAs) hybridisation or aptamers-based binding, each of which has high selectivity and sensitivity for the detection target (Labib et al., 2016). Then, the interactions are determined using measures of potential, current, ion concentration, conductance, capacitance or impedance changes (Felix and Angnes, 2018). Among them, label-free EISs have gained widespread attention because they are ultra-sensitive and can achieve rapid, electrochemical sensing and characterisation of various biological analytes, including virus antigens, antibodies and RNA (Faria and Zucolotto, 2019; Zhang and Miller, 2019).

One of the common types of label-free EISs is the impedimetric sensor. In impedimetric sensors, the interaction between target molecules and captured molecules at the electrode decreases the flux of the redox probe to the surface of the electrode and increases the impedance. These sensors exhibit high sensitivity for the detection of influenza virus antibodies and antigens (Chen et al., 2019; Zhang and Miller, 2019).

Table 3
Antibody-targeting SARS-COV-2 detection kits approved by the FDA.

Manufacturer	Type of antibody detected	Detection strategy	Detection method	Target	Sample volume	Detection system	Detection times	Sensitivity	Specificity
Bio-Rad Laboratories	Total Antibody	DASM:	ELISA	N	15 μL	Microplate reader equipped with 450 and 620 nm filters	120 min	Plasma: 83.33% (83.33%) Serum: 100% (27/27)	Plasma: 100% (75/75). Serum: 99.6% (543/545)
Abbott Laboratories Inc.	IgG	IAD	CMIA	N	25 μL	ARCHITECT i2000SR instrument or ARCHITECT i1000SR instrument		PPA; ˂14 days post-symptom onset : 61.7%; ≥14 days post-symptom onset: 96.77%	99.1%(111/112)
DiaSorin Inc.	IgG	IAD	CLI	S1 and S2	20 μL	LIAISON® XL Analyzer		≤ 5 days : 25% (11/44) 6–14 days: 89.80% (44/49) ≥15 days: 97.56% (40/41)	99.3% (1082/1090)
Ortho-Clinical Diagnostics, Inc	IgG	IAD	CLI	spike	20 μL	VITROS ECi/ECiQ/3600 Immunodiagnostic Systems and VITROS 5600/XT 7600 Integrated Systems	48 min	1–5 days*: 12/13; 6–15 days: 24/27; 16–22 days: 6/8	100%(407/407)
Autobio Diagnostics Co. Ltd.	IgM and IgG	IAD	ICGC	spike	5 μL	Not needed	15–20 min	IgM PPA: ≤7 days: 37.25%; 8–14 days: 73.08% ≥15 days: 95.70% IgG PPA: ≤7 days: 31.37%; 8–14 days: 65.38% ≥15 days: 99.01%	100%(189/189)
Mount Sinai Laboratory	IgG	IAD	ELISA	RBD	No mention	Microplate reader equipped with 490 and 620 nm filters	Not mentioned	PPA: 92% (37/40)	NPA: 100% (74/74)
Chembio Diagnostic System, Inc	IgM and IgG	IAD	ICGC	N	10 μl	Not needed	15–20 min	IgM: ≤6 days: 25% (1/4) 7–14 days: 71%(10/14) ≥15 days: 100%(13/13) IgG: ≤6 days: 100% (4/4) 7–14 days: 71%(10/14) ≥15 days: 100%(15/15)	IgM: 100% (49/49) IgG: 95.9% (47/49)
Ortho Clinical Diagnostics, Inc.	Total Antibody	DASM:	EPLCL	Spike	80 μL	ECi/ECiQ, 3600,5600, XT 7600	48 min	1–3 days[a]: 75%(6/8) 4–6 days: 77.7%(7/9) 7–9 days: 100%(2/2)	100%(400/400)
Cellex Inc.	IgM and IgG	IAD	ICGC	Not mentioned	10 μL	Not needed	15–20 min	PPA :93.75%	NPA: 96.40%

[a] Days between PCR positive and serum collection; PPA: positive percent agreement compared with RT-PCR results; NPA: negative percent agreement compared with RT-PCRrResults; RBD: receptor binding domain of spike protein; N: nucleocapsid protein; ELISA: Enzyme-Linked Immunosorbent Assay; CLI: chemiluminescent immunoassay; ICGC: immunocolloidal gold chromatography; EPLCL: enhance perioxidase/luminol chemiluminescence; CMIA: chemiluminescent microparticle immunoassay; IAD: indirect antibody detection; DASM: double-antigen sandwich methodology.

Cabral-Miranda et al. (2018) developed a carbon nanotube, electrode-based, impedimetric biosensor for detecting antibodies targeting the E protein and nonstructural protein 1 (NS1) with high sensitivity. This biosensor was reported to be 10,000 times more sensitive than ELISA. Moreover, impedimetric biosensors that achieve hypersensitive detection of nucleic acids have also been developed. For instance, Jayakumar et al. (2018) utilised co-electrodeposition of AuNPs and reduced graphene oxide (rGO) on a glassy carbon electrode (GCE) to prepare an electrochemical impedance DNA bioelectrode that can detect DNA hybridisation (LOD of 3.9×10^{-14} g/mL) with ultra-high sensitivity due to the increased amount of immobilised DNA and the highly selective hybridisation of gold nanoparticles (AuNPs). Similarly, Steinmetz et al. (2019) constructed a novel impedimetric biosensor by modifying an oxidised glassy carbon electrode with an AuNPs-3-n-propylpyridinium silsesquioxane polymer (SiPy) nanohybrid for detection of zika RNA; this biosensor had an LOD of 0.82 pmol/L.

Another promising type of label-free ElS is the field effect transistor, in which the binding of an analyte to the recognition element on the gate (G) terminal induces a charge distribution, produce a change in the surface potential which can finally lead to a measurable change in conductance between the source and the drain (Farka et al., 2017; Furst and Francis, 2019). Compared with other nanomaterial-based FET sensors, graphene and carbon nanotube-based FET sensors exhibit excellent electro-catalytic activity for high sensitivity detection, due to the unique physical, chemical, and electrical properties of carbon nanomaterials (Nehra and Pal Singh, 2015). Early on, Kim et al. (2013) described the scalable and facile fabrication of reduced graphene oxide FETs (R-GO FETs), in which an R-GO channel was formed by the reduction of graphene oxide nanosheets, networked by a self-assembly process. This FET was capable of label-free, ultrasensitive electrical detection of proteins, with an LOD as low as 100 fg/ml (1.1 fM). The upper detection limit was, however, down to 100 ng/mL, as higher density biomolecules near the R-GO surface in the human serum blocked analyte adsorption (Kim et al., 2013). Modification of graphene electronic devices, through patterned SAM arrays of hexamethyldisilazane, can enhance the electrical properties of G-FETs by providing a higher current on/off ratio and trans-conductance (Yeh et al., 2016). By virtue of this modified sensor, as few as 60 chondroitin sulfate proteoglycan 4 (0.01 fM) molecules could be detected in undiluted serum (Yeh et al., 2016). A recent study adopted crumpled graphene to increase the Debye length (e.g., shielding of the molecule charge by the counter ions in the solution); thereby enhancing the detection sensitivity of the graphene FET (Hwang et al., 2020). The further combination of the high DNA binding capacity of PNAs and the crumpled graphene FET showed ultra-high sensitivity nucleic acid detection in buffer and human serum samples, with LOD down to 600 zM and 20 aM, respectively, in a 1-h incubation time; these LODs are significantly lower than those of the flat, reduced graphene oxide FET biosensors (Cai et al., 2014; Hwang et al., 2020). This G-FET has been applied to highly sensitive virus antigen detection, such as detection of the ZIKA virus antigen NS1 and Ebola virus antigen glycoprotein (Afsahi et al., 2018; Maity et al., 2018). The high-sensitivity of G-FET was also recently used to detect SARS-CoV-2 virus particles in human NS specimens (Seo et al., 2020). Moreover, carbon nanotube-based FET sensors have shown great promise for the highly sensitive detection of virus antigens, antibodies, nucleic acids, and virus particles in clinical samples (Choi et al., 2017; Kim et al., 2020b; Mandal et al., 2012; Oh et al., 2013; Ramnani et al., 2013; Son et al., 2016).

8.3. Chip-based nucleic acid detection

Numerous efforts have been directed towards developing integrated Affordable, Sensitive, Specific, User-friendly, Rapid and robust, Equipment-free, and Deliverable (ASSURED) platforms for "sample-to-result" virus detection (Mauk et al., 2017). In particular, the development of ASSURED nucleic acid detection platforms is a great challenge because many steps, including cell or virus lysis, nucleic acid extraction and enrichment, and nucleic acid amplification or detection signal amplification, must be accomplished in a portable platform. Microfluidic technologies - "lab on chip" - have emerged as an attractive approach for nucleic acid-based testing at the point of care since microfluidic technologies offer highly-integrated disposable chips which allow potential automation from sample preparation to detection in inexpensive portable devices. In recent years, progress has been made with respect to making microfluidic devices which has enabled them to be more cost-effective with shorter test times using smaller sample and reagent volumes for virus detection in resource-limited settings (Mauk et al., 2017).

8.3.1. Pre-concentration of virus particles

The low load of SASR-CoV-2 in some patients is the main factor contributing to false-negative results. For this reason, it is better to pre-concentrate the virus from a large volume sample before nucleic acid extraction. For instance, Kim et al. (2020a) designed a microfluidic pre-concentration and nucleic amplification system (FPNAS) in which the anti-H1N1, antibody-conjugated, magnetic nanoparticles pre-concentrated the H1N1 virus from a large volume of saliva and, then, RT-PCR was used to detect the H1N1 virus. This approach improved the LOD by 10 orders of magnitude compared to non-treated samples (Fig. 6A). Hugle et al. (2020) developed a hydrogel chip for the pre-concentration of viral particles, which was then followed by thermal lysis and gel-electrophoretic nucleic acid extraction. In the pre-concentration process, negatively charged virus particles migrate towards the anode and accumulate at the separation gel (the blue line between the sample chamber and the elution chamber), in the middle of the chip, when a direct current (DC) voltage is applied between the anode (red) and the cathode (black) with a custom-made power supply (120 V) (Fig. 6B). Connelly et al. (2012) devised an integrated, microfluidic biosensor for virus concentration, wherein nanoporous membranes were fabricated in glass microchannels. In this biosensor, electrokinesis was adopted to concentrate the virus-antibody-liposome complex, followed by elution towards the capture bead bed (Fig. 6C).

8.3.2. Nucleic acid extraction and concentration in microfluidic chips

The major barrier for in-field nucleic acid detection is the shortage of cost-effective, simple cell or virus lysis and nucleic acid extraction methods. The cell lysis methods currently used in microfluidic systems include enzymatic lysis, chemical lysis, thermal lysis, electric cell lysis, and mechanical cell lysis (Zhu et al., 2020). Among them, chemical-enzyme combination lysis is a commonly used method in microfluidic detection. The commonly used filter membrane-based and magnetic bead-based nucleic acid extraction approach in microfluidic systems has been comprehensively reviewed and, thus, is not described in detail in this work (Mauk et al., 2017; Zhu et al., 2020). These two methods can extract and concentrate nucleic acids to increase the detection sensitivity of the system and are widely used in microfluidic, point-of-care applications. To further simplify the workflow of nucleic acid purification, isotachophoresis has been coupled into microfluidic chips to isolate and concentrate nucleic acids, where the electrophoretic mobility of nucleic acids is higher than the known impurities and downstream assay inhibitors (Qu et al., 2014; Rogacs et al., 2014). Hence, nucleic acids can be extracted and pre-concentrated in the presence of a leading electrolyte (LE) and a tailing electrolyte (TE) (Fig. 7A) (Subramanian Parimalam et al., 2018). Another nucleic acid extraction method is ion concentration polarization (ICP)-based electrokinetic (EK) trapping, in which the selective transport of cations through a cation-selective membrane (CEM), under a DC electric field, induces an ion depletion zone with significantly amplified electric fields in the microchannel; this acts as an electric force barrier that prevents the passage of negatively charged species (Ouyang et al., 2018). Negatively charged nucleic acids enter the microchannel by superposing an appropriate pressure-driven flow with an electroosmotic flow (EOF) under a tangential electric field, and these subsequently become trapped

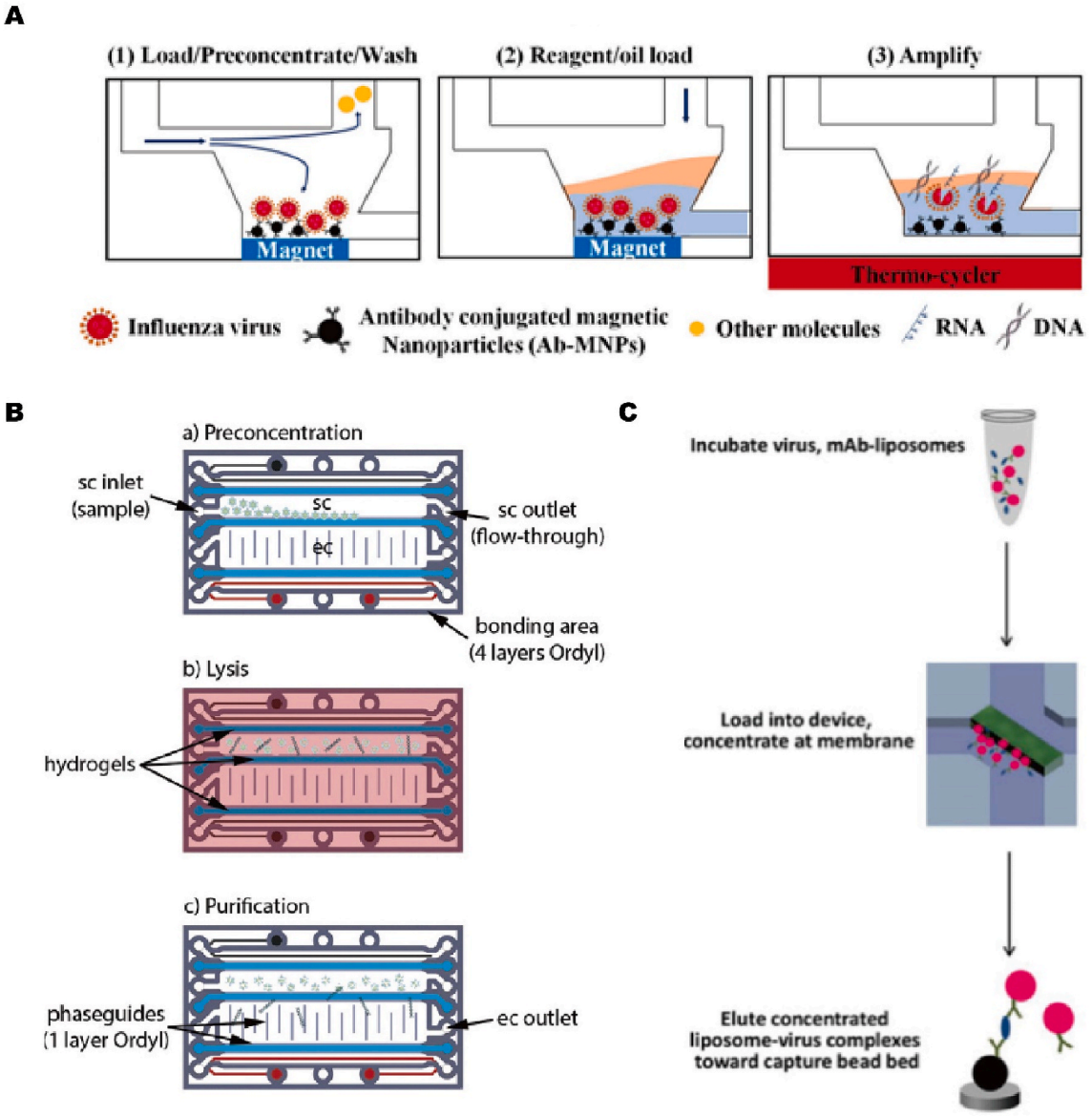

Fig. 6. (A) Schematic describing the operation protocol of on-chip pre-concentration and nucleic acid amplification. Reproduced with permission from (Kim et al., 2020a). (B) Workflow of free-flow electrophoretic virus particles at pre-concentration, followed by thermal lysis and gel-electrophoretic nucleic acid extraction. (a) Viruses (green) are captured in the sample chamber (sc) between the anode (red) and the cathode (black) at the separation gel (the blue line between sc and ec), using free-flow electrophoresis. (b) Thermal lysis of the concentrated viruses denatures the capsid, making the phage DNA accessible to electrophoretic transport. (c) Nucleic acids are transported through the separation gel into the elution chamber (ec) by gel electrophoresis (anode: red, cathode: black). Reproduced with permission from (Hugle et al., 2020). (C)Schematic illustration of electrokinetic pre-concentration (begins with loading the device with anti-FCV, pAb-labelled Protein A superparamagnetic beads to create a capture bed and incubating the anti-FCV mAb-labelled fluorescent liposomes with FCV). The sample is then loaded into the inlet well, concentrated at the nanoporous membrane, and eluted toward the capture bead bed. Reproduced with permission from (Connelly et al., 2012). (For interpretation of the references to colour in this figure legend, the reader is referred to the Web version of this article.)

at the electric force barrier within the microchannel, leading to the continuous concentration effect. On the other hand, proteins escape the ion depletion zone and leak downstream (Fig. 7B) (Ouyang et al., 2018). The coupling of hierarchically selective EK concentrations with microfluidic PCRs allow detection of the lowest number of detectable DNA copy numbers, five copies, which was two orders of magnitude better than the standard method (Ouyang and Han, 2019, 2020). In another study, Hügle et al. (2020) utilised gel electrophoresis to extract nucleic acids, i.e. the negatively charged DNA fragments moved to the positively charged anode from the sample chamber and then through the separation gel into the elution chamber. Intact phages and debris remained in the sample chamber, resulting in purification of the nucleic acids (Fig. 6B). Recently, Jin et al. (2017) combined dimethyl pimelimidate (DMP) and a low-cost, thin-film, microfluidic platform for the effective extraction of nucleic acids (both RNA and DNA), in which DMP could capture the nucleic acids by both electrostatic interaction and covalent bonding. Then, the complex binds to the thin film containing amine reactive groups in the microfluidic device. Finally, the elution buffer is added, to collect the extracted nucleic acids after washing in PBS twice, to remove the debris and unbound molecules (Fig. 7C).

8.3.3. *Nucleic acid detection in microfluidic systems*

Nucleic acid amplification tests (NAATs) have been widely coupled with microfluidic systems due to their high sensitivity and selectivity and their maturity as detection systems. Significant advancements have been made in terms of NAAT reagents and thermocycling instruments,

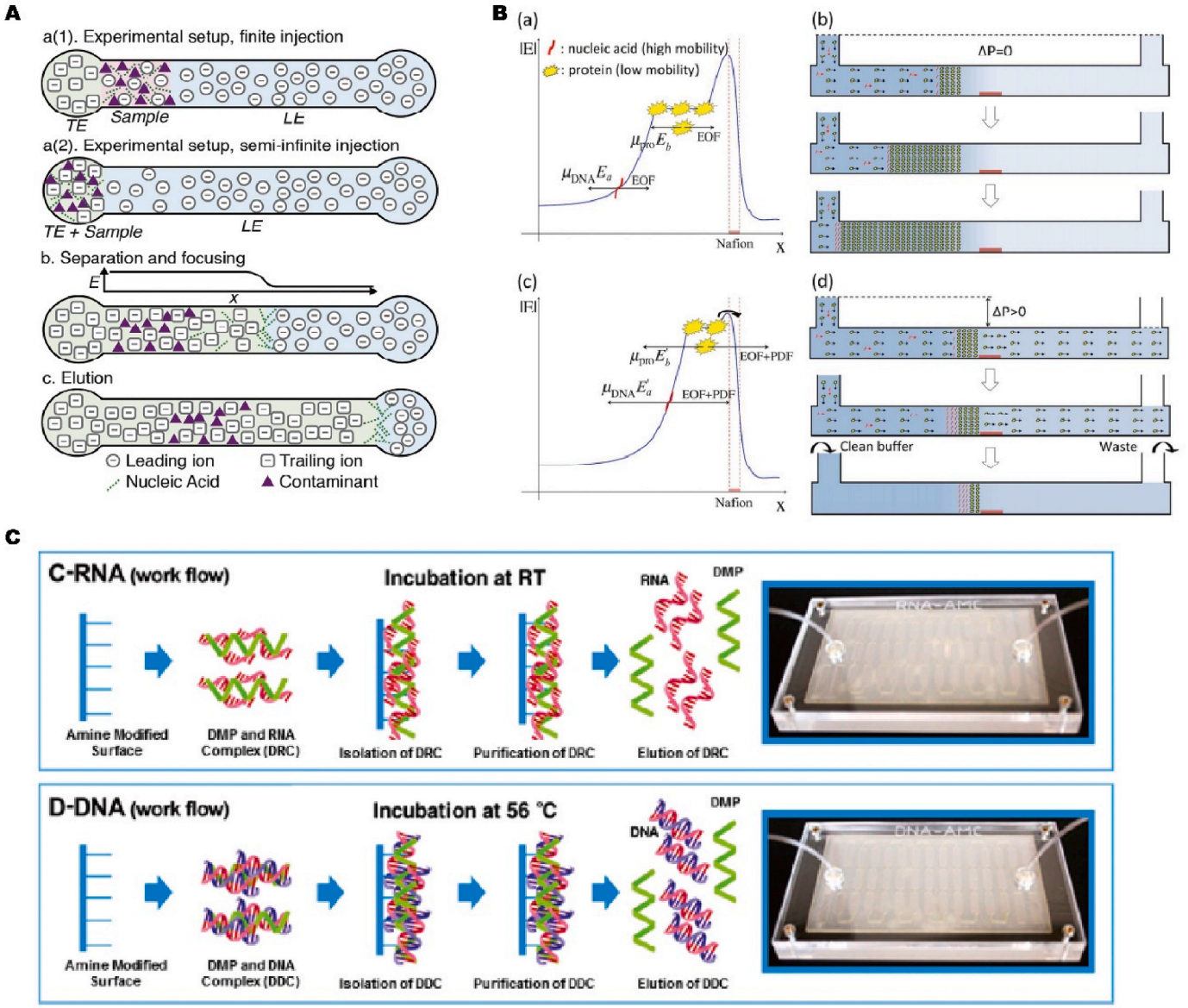

Fig. 7. (A) Schematic of the purification of nucleic acids using isotachophoresis. The purification can be initiated using at least two injection approaches. In the finite injection approach, (a1), the sample is injected into a channel and sandwiched between the trailing electrolyte (TE) and leading electrolyte (LE) regions that contain no samples. In the semi-infinite configuration approach, (a2), the sample is mixed into the TE reservoir. In either case, (b) the application of an electric current creates a steep electric field gradient at the TE-to-LE interface. NAs migrate faster than TE and accumulate at the TE-to-LE interface. The effective mobility of the TE anion is chosen to be higher than the mobilities of anionic impurities and, thus, impurities are gradually left behind. The NA eventually (c) elutes into the leading electrolyte reservoir, from which it can be extracted using a standard pipette for off-chip analysis. Reproduced with permission from (Rogacs et al., 2014). (B) Principle of PM-SET (a) The electrophoretic mobility of nucleic acids (NAs) is higher than that of proteins, so NAs concentrate farther from the Nafion membrane than proteins, where the electric field is weaker. (b) The concentration of proteins and NAs causes the rapid back-propagation of the NAs. (c) Under external hydrostatic pressure, proteins easily leak through the electric force barrier, while NAs are still effectively concentrated. (d) Under external hydrostatic pressure, NAs are stably concentrated near the ion depletion zone, while the background proteins are removed, enabling the simultaneous enrichment and purification of NAs. Reproduced with permission from (Ouyang et al., 2018). (C) The schematic of the Dimethyl Pimelimidate (DMP)-based Microfluidic System for extracting DNA or RNA. A mixture solution, including lysis buffer, samples, and DMP, is incubated at either RT for 10–20 min (for RNA) or 56 °C for 20 min (for DNA) to capture RNA or DNA through the DMP reagent on the amine modified surface of the thin film. Finally, the nucleic acids (RNA or DNA) are quickly washed and eluted. Reproduced with permission from (Jin et al., 2017).

and these have improved the heat transfer rate of NAATs, contributing to ultrafast, sample-to-answer, nucleic acid POCT detection (Lee et al., 2019). However, due to their cost and complexity, their widespread application is limited, especially in areas with limited resources.

Among the available NAATs, isothermal nucleic acid amplification tests (iNAATs) without an initial heating step (~95 °C) to denature dsDNA are ideal candidates for POCT applications (Lee et al., 2019). One promising iNAAT is LAMP, which has been widely used for POCT SARS-CoV-2 detection (Table 3). In addition, LAMP is the most common iNAAT adopted in microfluidic NAATs. Previously, Wang et al. (2011) presented an integrated microfluidic LAMP lab-on-a-chip (LOC) system to automatically complete the thermal lysis, RNA extraction, and RNA amplification. In this system, nervous necrosis virus RNA is captured and concentrated using magnetic nanoparticles after thermal lysis. Then, a one-step RT-LAMP reagent is loaded to perform the subsequent simultaneous synthesis of cDNA and isothermal amplification (Fig. 8A). Liu

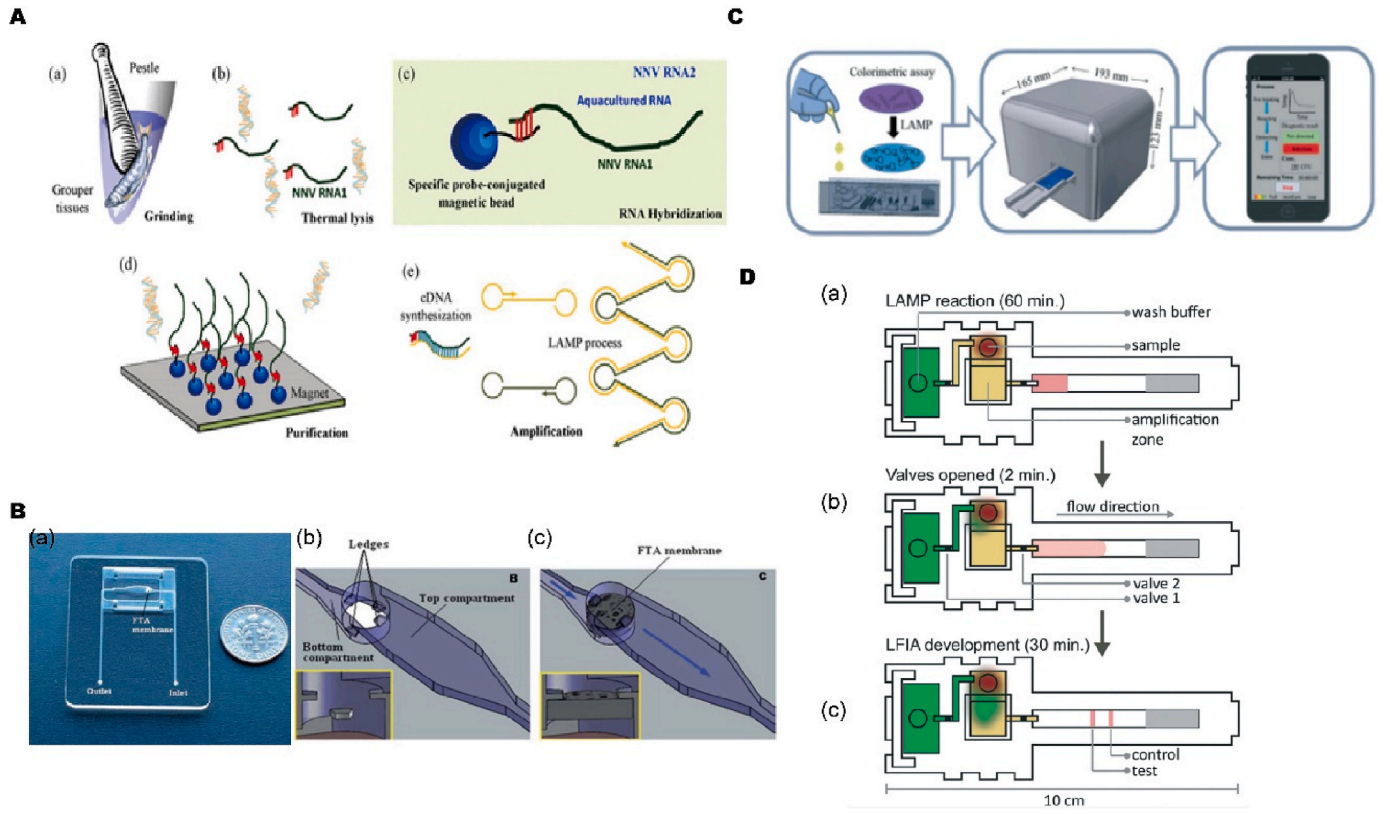

Fig. 8. (A) Schematic illustrations of the experimental process of rapid RNA purification and NNV detection using an integrated microfluidic LAMP system. Reproduced with permission from (Wang et al., 2011). (B) Experimental workflow of a sample-to-answer, potable platform for rapid pathogen detection. Reproduced with permission from (Ma et al., 2019). (C) Schematic illustrations of a single-chamber, microfluidic cassette with an integrated FTA membrane (a) A photograph. (b) An amplified view of the reaction chamber without the FTA membrane. Two sets of protruding ledges are machined on the top and bottom of the LAMP chamber. (c) An amplified view of the reaction chamber with the installed FTA membrane, which separates the reaction chamber into a top main compartment and a bottom compartment. Reproduced with permission from (Liu et al., 2011). (D) Schematic of fluid travel through microRAAD. (a) The wash buffer (green) is constrained from flowing to the amplification zone and the sample (red blood cells and yellow plasma) is constrained from flowing to the LFIA by closed valves. (b) Upon thermally actuating the valves, wash buffer is released to the amplification zone and the RT-LAMP products migrate to the LFIA for (c) test band development. Reproduced with permission from (Phillips et al., 2019). (For interpretation of the references to colour in this figure legend, the reader is referred to the Web version of this article.)

et al. (2011) devised a single-chamber LAMP cassette system in which a Flinders Technology Associates (Whatman FTA®) membrane is installed at the interface, between the inlet port and the reaction chamber, to purify nucleic acids, block the introduction of air bubbles into the reaction chamber, remove amplification inhibitors from the saliva sample, and finally, improve the detection limit (Fig. 8B). The single-chamber LAMP cassette system can detect human immunodeficiency virus type 1 (HIV-1) in oral fluid, with a sensitivity of 10 HIV particles per reaction chamber, within 27 min (Liu et al., 2011). Recently, a smartphone-based "sample-to-answer" portable system integrated with a self-driven passive microfluidic device was developed (Ma et al., 2019). In this system, hydrophobic soft valves were inserted in the downstream end of each reservoir to block liquid flow, which can be stopped and resumed by stopping and resuming a punching-press mechanism (Fig. 8C). In this way, the virus pre-concentration, virus lysis, RNA extraction, and LAMP detection processes can be automatically completed in 40 min. Finally, colorimetric assays have been used to detect influenza A virus, with limits of 3.2×10^{-3} hemagglutinating units (HAU) per reaction. Phillips et al. (2019) designed a microfluidic rapid and autonomous analytical device (microRAAD) which can leverage the wicking abilities of paper membranes and size discriminating pores to isolate HIV virus particles from human blood cells and then utilises pre-dried RT-LAMP reagents to amplify RNA from the virus particles (Fig. 8D). The RT-LAMP amplicons are automatically transported to an integrated LFIA for simple visual interpretation of the results. The detection process is completed in 90 min, with a LOD of 3×10^5 HIV-1 viral particles or 2.3×10^7 virus copies/mL.

Another promising iNAAT, the recombinase polymerase amplification (RPA), is performed entirely at a relatively low temperature, ranging from ~37 °C to ~42 °C. RPA has several advantages, including fast reaction time with relaxed requirements for temperature control. Portable sophisticated fluorescence sensors and a commercial TwistAmp RT exo kit are available for the development of nucleic acid detection assays (Euler et al., 2012). Using the above materials and sensor, high sensitivity detection kits have been prepared for detecting RNA viruses, such as Avian Influenza H5N1 (LOD: 1copy, 20 min) (Yehia et al., 2015), MERS-CoV (LOD: 10 copies, 10 min) (Abd El Wahed et al., 2013), and Ebola Virus (LOD: 5 copies, 10 min) (Faye et al., 2015). Combined with magnetic nanoparticle nucleic acid extraction, the LOD of H7N9 detection reached 10 copies in 2–7 min (Abd El Wahed et al., 2015). In addition, many researchers have devoted great efforts to integrating RPA into a microfluidic chip. Lutz et al. (2010) first integrated RPA with a centrifugal microfluidic cartridge for the rapid detection of the antibiotic resistance gene *mecA* of Staphylococcus aureus. This system had LOD of ˂10 copies in 20 min. Subsequently, Kim et al. (2014) created a micro total analysis system which integrated DNA extraction, RPA, and LFA detection onto a single disc. To further increase the detection sensitivity, Yang et al. (2018) built an integrated sample-in-digital-answer-out (SIDAO) disposable cartridge incorporating DNA extraction and digital recombinase polymerase amplification (dRPA) which can enable rapid and absolute quantitative nucleic acid analysis. Recently, Yin et al. (2020) described an integrated

multiplex dRPA microfluidic chip which can simultaneously detect three species of pathogenic bacteria within 45 min. Furthermore, the DNA amplification of RPA can be monitored in real-time using a low cost thin-film transistor (TFT) nanoribbon (NR) sensor (C. Hu et al., 2017; L. M. Hu et al., 2017). The principle of this system is the incorporation of a single nucleotide into a DNA strand, thus releasing protons and acidifying the suspended electrolyte during DNA amplification. Recombinase then binds cooperatively to the primer (oligonucleotides), inducing ATP conversion to ADP, with the generation of H^+ (C. Hu et al., 2017; L. M. Hu et al., 2017). Using this method, < 10 copies of genomic DNA could be detected in 5 min, with significantly higher sensitivity and much quicker processing time than fluorescence assays (C. Hu et al., 2017; L. M. Hu et al., 2017).

9. Conclusion

In conclusion, nucleic acid and antibody detection assays play important roles in the rapid identification and isolation of COVID-19 patients to reduce further spread of SARS-CoV-2 infection. However, the current SARS-CoV-2 RNA detection assays have some limitations, including low detection sensitivity, long detection times, the need to extract RNA from clinical samples, the frequent false-negative nucleic acid results obtained in clinical applications, and the need to be performed by professional technicians. Therefore, patients with low level of SARS-CoV-2 RNA are very likely be missed. Other potential biomarkers for early screening of COVID-19 patients, including the NP antigen and SARS-CoV-2 virus particles, are present at low levels in body fluid, making point-of-care detection challenging. To date, there is no commercially-available antigen or virus detection kit, and the early diagnostic value of NP antigen detection is still elusive. In addition, patients exhibit low levels of antibodies targeting SARS-CoV-2 during the early period of infection. Therefore, the widely-used, low-sensitivity antibody detection method, CGLFA had low detection rate in the early COVID-19 patients.

10. Future perspectives

With regards to SARS-CoV-2 RNA detection, more work is needed to achieve simple, highly effective release and enrichment of SARS-CoV-2 RNA from clinical samples for direct amplification. Further, the combination of efficient isothermal RNA amplification and high sensitivity detection technologies (such as electrochemical biosensors) is needed for rapid, real-time, highly sensitive detection of SARS-CoV-2 RNA. The present review highlighted that biosensors have great potential for rapid, high-sensitivity, in-field SARS-CoV-2 RNA detection. In these biosensors, virus enrichment, RNA extraction and concentration, and RNA amplification and detection could be integrated into disposable sensors, such as microfluidic chips, for sample-to-result SARS-CoV-2 RNA detection (Kant et al., 2018).

Given that it usually takes 1–2 weeks for human B cells to produce and secrete commonly-detectable antibodies into the serum after virus infection, therefore, there is a low level of serum antibodies in the early stage of COVID-19 infection (Long et al., 2020), SARS-CoV-2 NP and virus particle detection are the best potential methods for providing direct early proof of SARS-CoV-2 infection. Detection of these two biomarkers could be the optimal strategy for early point-of-care screening of potential COVID-19 patients. However, the SARS-CoV-2 NP and virus particle are also low in the body fluids of COVID-19 patients (L. Pan et al., 2020; Y. Pan et al., 2020; Lv et al., 2020). Therefore, novel, promising, high-sensitivity POCT immunosensors, such as NIR emitting nanoparticles, magnetic nanoparticle-based LFAs, and electrochemical biosensors, deserve further exploration for their role in improving anti-SP, anti-NP antibody, SARS-CoV-2 NP antigen, and virus particle detection assays.

Declaration of competing interest

The authors declare that they have no known competing financial interests or personal relationships that could have appeared to influence the work reported in this paper.

Acknowledgements

This work was supported by the National Natural Science Foundation of China (81673040), Guangdong Provincial Department of Education Youth innovative talents Project (2017KQNCX168) and Guangzhou Science and Technology Project (201904010214). Guangzhou Health technology General guidance project (20201A011078).

Appendix A. Supplementary data

Supplementary data to this article can be found online at https://doi.org/10.1016/j.bios.2020.112455.

References

Abd El Wahed, A., Patel, P., Heidenreich, D., Hufert, F.T., Weidmann, M., 2013. Reverse transcription recombinase polymerase amplification assay for the detection of middle East respiratory syndrome coronavirus. PLoS Curr. 5.

Abd El Wahed, A., Weidmann, M., Hufert, F.T., 2015. Diagnostics-in-a-Suitcase: development of a portable and rapid assay for the detection of the emerging avian influenza A (H7N9) virus. J. Clin. Virol. 69, 16–21.

Afsahi, S., Lerner, M.B., Goldstein, J.M., Lee, J., Tang, X., Bagarozzi Jr., D.A., Pan, D., Locascio, L., Walker, A., Barron, F., Goldsmith, B.R., 2018. Novel graphene-based biosensor for early detection of Zika virus infection. Biosens. Bioelectron. 100, 85–88.

Ai, J.W., Zhang, Y., Zhang, H.C., Xu, T., Zhang, W.H., 2020. Era of molecular diagnosis for pathogen identification of unexplained pneumonia, lessons to be learned. Emerg. Microb. Infect. 9 (1), 597–600.

Azzi, L., Carcano, G., Gianfagna, F., Grossi, P., Gasperina, D.D., Genoni, A., Fasano, M., Sessa, F., Tettamanti, L., Carinci, F., Maurino, V., Agostino, R., Tagliabue, A., University of Insubria, C.-T.F., Baj, A., 2020. SALIVA IS A RELIABLE TOOL TO DETECT SARS-CoV-2. J. Infect. 81 (1), e45–e50.

Backer, J.A., Klinkenberg, D., Wallinga, J., 2020. Incubation period of 2019 novel coronavirus (2019-nCoV) infections among travellers from Wuhan, China, 20-28 January 2020. Euro Surveill. 25 (5), 2000062.

Baek, Y.H., Um, J., Antigua, K.J.C., Park, J.H., Kim, Y., Oh, S., Kim, Y.I., Choi, W.S., Kim, S.G., Jeong, J.H., Chin, B.S., Nicolas, H.D.G., Ahn, J.Y., Shin, K.S., Choi, Y.K., Park, J.S., Song, M.S., 2020. Development of a reverse transcription-loop-mediated isothermal amplification as a rapid early-detection method for novel SARS-CoV-2. Emerg. Microb. Infect. 9 (1), 998–1007.

Bloch, E.M., Shoham, S., Casadevall, A., Sachais, B.S., Shaz, B., Winters, J.L., van Buskirk, C., Grossman, B.J., Joyner, M., Henderson, J.P., Pekosz, A., Lau, B., Wesolowski, A., Katz, L., Shan, H., Auwaerter, P.G., Thomas, D., Sullivan, D.J., Paneth, N., Gehrie, E., Spitalnik, S., Hod, E., Pollack, L., Nicholson, W.T., Pirofski, L. A., Bailey, J.A., Tobian, A.A., 2020. Deployment of convalescent plasma for the prevention and treatment of COVID-19. J. Clin. Invest. 130 (6), 2757–2765.

Bordi, L., Nicastri, E., Scorzolini, L., Di Caro, A., Capobianchi, M.R., Castilletti, C., Lalle, E., On Behalf Of Inmi Covid-Study, G., Collaborating, C., 2020. Differential diagnosis of illness in patients under investigation for the novel coronavirus (SARS-CoV-2), Italy. February 2020 Euro Surveill. 25 (8), 2000170.

Broughton, J.P., Deng, X., Yu, G., Fasching, C.L., Servellita, V., Singh, J., Miao, X., Streithorst, J.A., Granados, A., Sotomayor-Gonzalez, A., Zorn, K., Gopez, A., Hsu, E., Gu, W., Miller, S., Pan, C.Y., Guevara, H., Wadford, D.A., Chen, J.S., Chiu, C.Y., 2020. CRISPR-Cas12-based detection of SARS-CoV-2. Nat. Biotechnol. 38 (7), 870–874.

Cabral-Miranda, G., Cardoso, A.R., Ferreira, L.C.S., Sales, M.G.F., Bachmann, M.F., 2018. Biosensor-based selective detection of Zika virus specific antibodies in infected individuals. Biosens. Bioelectron. 113, 101–107.

Cai, X.F., Chen, J., Li, H.J., Long, Q.X., Deng, H.J., Liu, P., Fan, K., Liao, P., Liu, B.Z., Wu, G.C., Chen, Y.K., Li, Z.J., Wang, K., Zhang, X.L., Tian, W.G., Xiang, J.L., Du, H. X., Wang, J., Hu, Y., Tang, N., Lin, Y., Ren, J.H., Huang, L.Y., Wei, J., Gan, C.Y., Chen, Y.M., Gao, Q.Z., Chen, A.M., He, C.L., Wang, D.X., Hu, P., Zhou, F.C., Huang, A.L., Wang, D.Q., 2020. A peptide-based magnetic chemiluminescence enzyme immunoassay for serological diagnosis of coronavirus disease 2019. J. Infect. Dis. 222 (2), 189–193.

Cai, B., Wang, S., Huang, L., Ning, Y., Zhang, Z., Zhang, G.J., 2014. Ultrasensitive label-free detection of PNA-DNA hybridization by reduced graphene oxide field-effect transistor biosensor. ACS Nano 8 (3), 2632–2638.

Chan, J.F., Kok, K.H., Zhu, Z., Chu, H., To, K.K., Yuan, S., Yuen, K.Y., 2020a. Genomic characterization of the 2019 novel human-pathogenic coronavirus isolated from a patient with atypical pneumonia after visiting Wuhan. Emerg. Microb. Infect. 9 (1), 221–236.

Chan, J.F., Yip, C.C., To, K.K., Tang, T.H., Wong, S.C., Leung, K.H., Fung, A.Y., Ng, A.C., Zou, Z., Tsoi, H.W., Choi, G.K., Tam, A.R., Cheng, V.C., Chan, K.H., Tsang, O.T.,

Yuen, K.Y., 2020b. Improved molecular diagnosis of COVID-19 by the novel, highly sensitive and specific COVID-19-RdRp/Hel real-time reverse transcription-PCR assay validated in vitro and with clinical specimens. J. Clin. Microbiol. 58 (5), e00310–e00320.
Che, X.Y., Hao, W., Wang, Y., Di, B., Yin, K., Xu, Y.C., Feng, C.S., Wan, Z.Y., Cheng, V.C., Yuen, K.Y., 2004. Nucleocapsid protein as early diagnostic marker for SARS. Emerg. Infect. Dis. 10 (11), 1947–1949.
Chen, X., Dong, T., Wei, X., Yang, Z., Matos Pires, N.M., Ren, J., Jiang, Z., 2019. Electrochemical methods for detection of biomarkers of Chronic Obstructive Pulmonary Disease in serum and saliva. Biosens. Bioelectron. 142, 111453.
Choi, J., Seong, T.W., Jeun, M., Lee, K.H., 2017. Field-effect biosensors for on-site detection: recent advances and promising targets. Adv. Healthc. Mater. 6 (20).
Chu, D.K.W., Pan, Y., Cheng, S.M.S., Hui, K.P.Y., Krishnan, P., Liu, Y., Ng, D.Y.M., Wan, C.K.C., Yang, P., Wang, Q., Peiris, M., Poon, L.L.M., 2020. Molecular diagnosis of a novel coronavirus (2019-nCoV) causing an outbreak of pneumonia. Clin. Chem. 66 (4), 549–555.
Connelly, J.T., Kondapalli, S., Skoupi, M., Parker, J.S., Kirby, B.J., Baeumner, A.J., 2012. Micro-total analysis system for virus detection: microfluidic pre-concentration coupled to liposome-based detection. Anal. Bioanal. Chem. 402 (1), 315–323.
Corman, V.M., Landt, O., Kaiser, M., Molenkamp, R., Meijer, A., Chu, D.K., Bleicker, T., Brunink, S., Schneider, J., Schmidt, M.L., Mulders, D.G., Haagmans, B.L., van der Veer, B., van den Brink, S., Wijsman, L., Goderski, G., Romette, J.L., Ellis, J., Zambon, M., Peiris, M., Goossens, H., Reusken, C., Koopmans, M.P., Drosten, C., 2020. Detection of 2019 novel coronavirus (2019-nCoV) by real-time RT-PCR. Euro Surveill. 25 (3), 2000045.
Dai, Y., Liu, C.C., 2019. Recent advances on electrochemical biosensing strategies toward universal point-of-care systems. Angew. Chem. 58 (36), 12355–12368.
Das, D., Kammila, S., Suresh, M.R., 2010. Development, characterization, and application of monoclonal antibodies against severe acute respiratory syndrome coronavirus nucleocapsid protein. Clin. Vaccine Immunol. : CVI 17 (12), 2033–2036.
Diao, B., Wen, K., Chen, J., Liu, Y., Yuan, Z., Han, C., Chen, J., Pan, Y., Chen, L., Dan, Y., Wang, J., Chen, Y., Deng, G., Zhou, H., Wu, Y., 2020. Diagnosis of Acute Respiratory Syndrome Coronavirus 2 Infection by Detection of Nucleocapsid Protein. medRxiv.
Dincer, C., Bruch, R., Costa-Rama, E., Fernandez-Abedul, M.T., Merkoci, A., Manz, A., Urban, G.A., Guder, F., 2019. Disposable sensors in diagnostics, food, and environmental monitoring. Adv. Mater. 31 (30), e1806739.
Ding, X., Yin, K., Li, Z., Liu, C., 2020. All-in-One Dual CRISPR-Cas12a (AIOD-CRISPR) Assay: A Case for Rapid, Ultrasensitive and Visual Detection of Novel Coronavirus SARS-CoV-2 and HIV Virus. bioRxiv.
Du, Z., Xu, X., Wu, Y., Wang, L., B, J., C, L., A, M., 2020. Serial interval of COVID-19 from publicly reported confirmed cases. Emerg. Infect. Dis. 26 (6), 1341–1343.
Escors, D., Ortego, J., Laude, H., Enjuanes, L., 2001. The membrane M protein carboxy terminus binds to transmissible gastroenteritis coronavirus core and contributes to core stability. J. Virol. 75 (3), 1312–1324.
Euler, M., Wang, Y., Nentwich, O., Piepenburg, O., Hufert, F.T., Weidmann, M., 2012. Recombinase polymerase amplification assay for rapid detection of Rift Valley fever virus. J. Clin. Virol. 54 (4), 308–312.
Faria, H.A.M., Zucolotto, V., 2019. Label-free electrochemical DNA biosensor for zika virus identification. Biosens. Bioelectron. 131, 149–155.
Farka, Z., Jurik, T., Kovar, D., Trnkova, L., Skladal, P., 2017. Nanoparticle-based immunochemical biosensors and assays: recent advances and challenges. Chem. Rev. 117 (15), 9973–10042.
Faye, O., Faye, O., Soropogui, B., Patel, P., El Wahed, A.A., Loucoubar, C., Fall, G., Kiory, D., Magassouba, N., Keita, S., Konde, M.K., Diallo, A.A., Koivogui, L., Karlberg, H., Mirazimi, A., Nentwich, O., Piepenburg, O., Niedrig, M., Weidmann, M., Sall, A.A., 2015. Development and deployment of a rapid recombinase polymerase amplification Ebola virus detection assay in Guinea in 2015. Euro Surveill. 20 (44), pii=30053.
Felix, F.S., Angnes, L., 2018. Electrochemical immunosensors - a powerful tool for analytical applications. Biosens. Bioelectron. 102, 470–478.
Furst, A.L., Francis, M.B., 2019. Impedance-based detection of bacteria. Chem. Rev. 119 (1), 700–726.
Guo, X., Guo, Z., Duan, C., Chen, Z., Wang, G., Lu, Y., Li, M., Lu, J., 2020a. Long-Term Persistence of IgG Antibodies in SARS-CoV Infected Healthcare Workers. medRxiv.
Guo, L., Ren, L., Yang, S., Xiao, M., Chang, Yang, F., Dela Cruz, C.S., Wang, Y., Wu, C., Xiao, Y., Zhang, L., Han, L., Dang, S., Xu, Y., Yang, Q., Xu, S., Zhu, H., Xu, Y., Jin, Q., Sharma, L., Wang, L., Wang, J., 2020b. Profiling early humoral response to diagnose novel coronavirus disease (COVID-19). Clin. Infect. Dis. ciaa310.
He, H., Li, R., Chen, Y., Pan, P., Tong, W., Dong, X., Chen, Y., Yu, D., 2017. Integrated DNA and RNA extraction using magnetic beads from viral pathogens causing acute respiratory infections. Sci. Rep. 7, 45199.
Hellewell, J., Abbott, S., Gimma, A., Bosse, N.I., Jarvis, C.I., Russell, T.W., Munday, J.D., Kucharski, A.J., Edmunds, W.J., Centre for the Mathematical Modelling of Infectious Diseases COVID-19 Working Group, Funk, S., Eggo, R.M., 2020. Lancet Glob. Health 8 (4), e488–e496.
Hoffmann, M., Kleine-Weber, H., Schroeder, S., Kruger, N., Herrler, T., Erichsen, S., Schiergens, T.S., Herrler, G., Wu, N.H., Nitsche, A., Muller, M.A., Drosten, C., Pohlmann, S., 2020. SARS-CoV-2 cell entry depends on ACE2 and TMPRSS2 and is blocked by a clinically proven protease inhibitor. Cell 181 (2), 271–280 e278.
Hou, T., Zeng, W., Yang, M., Chen, W., Ren, L., Ai, J., Wu, J., Liao, Y., Gou, X., Li, Y., Wang, X., Su, H., Gu, B., Wang, J., Xu, T., 2020. Development and Evaluation of A CRISPR-Based Diagnostic for 2019-novel Coronavirus. medRxiv.
Huang, W.E., Lim, B., Hsu, C.C., Xiong, D., Wu, W., Yu, Y., Jia, H., Wang, Y., Zeng, Y., Ji, M., Chang, H., Zhang, X., Wang, H., Cui, Z., 2020. RT-LAMP for rapid diagnosis of coronavirus SARS-CoV-2. Microb. Biotechnol. 13 (4), 950–961.
Hu, C., Kalsi, S., Zeimpekis, I., Sun, K., Ashburn, P., Turner, C., Sutton, J.M., Morgan, H., 2017a. Ultra-fast electronic detection of antimicrobial resistance genes using isothermal amplification and Thin Film Transistor sensors. Biosens. Bioelectron. 96, 281–287.
Hu, L.M., Luo, K., Xia, J., Xu, G.M., Wu, C.H., Han, J.J., Zhang, G.G., Liu, M., Lai, W.H., 2017b. Advantages of time-resolved fluorescent nanobeads compared with fluorescent submicrospheres, quantum dots, and colloidal gold as label in lateral flow assays for detection of ractopamine. Biosens. Bioelectron. 91, 95–103.
Huang, X., Aguilar, Z.P., Xu, H., Lai, W., Xiong, Y., 2016. Membrane-based lateral flow immunochromatographic strip with nanoparticles as reporters for detection: a review. Biosens. Bioelectron. 75, 166–180.
Hugle, M., Behrmann, O., Raum, M., Hufert, F.T., Urban, G.A., Dame, G., 2020. A lab-on-a-chip for free-flow electrophoretic preconcentration of viruses and gel electrophoretic DNA extraction. Analyst 145 (7), 2554–2561.
Hwang, M.T., Heiranian, M., Kim, Y., You, S., Leem, J., Taqieddin, A., Faramarzi, V., Jing, Y., Park, I., van der Zande, A.M., Nam, S., Aluru, N.R., Bashir, R., 2020. Ultrasensitive detection of nucleic acids using deformed graphene channel field effect biosensors. Nat. Commun. 11 (1), 1543.
Ihling, C., Tänzler, D., Hagemann, S., Kehlen, A., Hüttelmaier, S., Sinz, A., 2020. Mass Spectrometric Identification of SARS-CoV-2 Proteins from Gargle Solution Samples of COVID-19 Patients bioRxiv.
Jayakumar, K., Camarada, M.B., Dharuman, V., Ju, H., Dey, R.S., Wen, Y., 2018. One-step coelectrodeposition-assisted layer-by-layer assembly of gold nanoparticles and reduced graphene oxide and its self-healing three-dimensional nanohybrid for an ultrasensitive DNA sensor. Nanoscale 10 (3), 1196–1206.
Jin, C.E., Koo, B., Lee, T.Y., Han, K., Lim, S.B., Park, I.J., Shin, Y., 2018. Simple and low-cost sampling of cell-free nucleic acids from blood plasma for rapid and sensitive detection of circulating tumor DNA. Adv. Sci. 5 (10), 1800614.
Jin, C.E., Lee, T.Y., Koo, B., Choi, K.C., Chang, S., Park, S.Y., Kim, J.Y., Kim, S.H., Shin, Y., 2017. Use of dimethyl pimelimidate with microfluidic system for nucleic acids extraction without electricity. Anal. Chem. 89 (14), 7502–7510.
Kant, K., Shahbazi, M.A., Dave, V.P., Ngo, T.A., Chidambara, V.A., Than, L.Q., Bang, D. D., Wolff, A., 2018. Microfluidic devices for sample preparation and rapid detection of foodborne pathogens. Biotechnol. Adv. 36 (4), 1003–1024.
Kim, D.J., Sohn, I.Y., Jung, J.H., Yoon, O.J., Lee, N.E., Park, J.S., 2013. Reduced graphene oxide field-effect transistor for label-free femtomolar protein detection. Biosens. Bioelectron. 41, 621–626.
Kim, Y., Abafogi, A.T., Tran, B.M., Kim, J., Lee, J., Chen, Z., Bae, P.K., Park, K., Shin, Y. B., van Noort, D., Lee, N.Y., Park, S., 2020a. Integrated microfluidic preconcentration and nucleic amplification system for detection of influenza A virus H1N1 in saliva. Micromachines 11 (2), 203.
Kim, K., Kim, M.J., Kim, D.W., Kim, S.Y., Park, S., Park, C.B., 2020b. Clinically accurate diagnosis of Alzheimer's disease via multiplexed sensing of core biomarkers in human plasma. Nat. Commun. 11 (1), 119.
Kim, J., Kwon, J.H., Jang, J., Lee, H., Kim, S., Hahn, Y.K., Kim, S.K., Lee, K.H., Lee, S., Pyo, H., Song, C.S., Lee, J., 2018. Rapid and background-free detection of avian influenza virus in opaque sample using NIR-to-NIR upconversion nanoparticle-based lateral flow immunoassay platform. Biosens. Bioelectron. 112, 209–215.
Kim, D., Lee, J.Y., Yang, J.S., Kim, J.W., Kim, V.N., Chang, H., 2020c. The architecture of SARS-CoV-2 transcriptome. Cell 181 (4), 914–921.
Kim, T.H., Park, J., Kim, C.J., Cho, Y.K., 2014. Fully integrated lab-on-a-disc for nucleic acid analysis of food-borne pathogens. Anal. Chem. 86 (8), 3841–3848.
Kimball, A., Hatfield, K.M., Arons, M., James, A., Taylor, J., Spicer, K., Bardossy, A.C., Oakley, L.P., Tanwar, S., Chisty, Z., Bell, J.M., Methner, M., Harney, J., Jacobs, J.R., Carlson, C.M., McLaughlin, H.P., Stone, N., Clark, S., Brostrom-Smith, C., Page, L.C., Kay, M., Lewis, J., Russell, D., Hiatt, B., Gant, J., Duchin, J.S., Clark, T.A., Honein, M. A., Reddy, S.C., Jernigan, J.A., Public Health, S., King, C., Team, C.C.-I., 2020. Asymptomatic and presymptomatic SARS-CoV-2 infections in residents of a long-term care skilled nursing facility - king county, Washington, march 2020. MMWR (Morb. Mortal. Wkly. Rep.) 69 (13), 377–381.
Labib, M., Sargent, E.H., Kelley, S.O., 2016. Electrochemical methods for the analysis of clinically relevant biomolecules. Chem. Rev. 116 (16), 9001–9090.
Lau, S.K., Che, X.Y., Woo, P.C., Wong, B.H., Cheng, V.C., Woo, G.K., Hung, I.F., Poon, R. W., Chan, K.H., Peiris, J.S., Yuen, K.Y., 2005. SARS coronavirus detection methods. Emerg. Infect. Dis. 11 (7), 1108–1111.
Lauer, S.A., Grantz, K.H., Bi, Q., Jones, F.K., Zheng, Q., Meredith, H.R., Azman, A.S., Reich, N.G., Lessler, J., 2020. The incubation period of coronavirus disease 2019 (COVID-19) from publicly reported confirmed cases: estimation and application. Ann. Intern. Med. 172 (9), 577–582.
Lee, S.H., Park, S.M., Kim, B.N., Kwon, O.S., Rho, W.Y., Jun, B.H., 2019. Emerging ultrafast nucleic acid amplification technologies for next-generation molecular diagnostics. Biosens. Bioelectron. 141, 111448.
Li, M., Jin, R., Peng, Y., Wang, C., Ren, W., Lv, F., Gong, S., Fang, F., Wang, Q., Li, J., Shen, T., Sun, H., Zhou, L., Cui, Y., Song, H., Sun, L., 2020b. Generation of Antibodies against COVID-19 Virus for Development of Diagnostic Tools. medRxiv.
Li, R., Pei, S., Chen, B., Song, Y., Zhang, T., Yang, W., Shaman, J., 2020. Substantial undocumented infection facilitates the rapid dissemination of novel coronavirus (SARS-CoV2). Science 368 (6490), 489–493.
Li, Z., Yi, Y., Luo, X., Xiong, N., Liu, Y., Li, S., Sun, R., Wang, Y., Hu, B., Chen, W., Zhang, Y., Wang, J., Huang, B., Lin, Y., Yang, J., Cai, W., Wang, X., Cheng, J., Chen, Z., Sun, K., Pan, W., Zhan, Z., Chen, L., Ye, F., 2020a. Development and clinical application of a rapid IgM-IgG combined antibody test for SARS-CoV-2 infection diagnosis. J. Med. Virol. 1–7.
Liang, W.H., Guan, W.J., Li, C.C., Li, Y.M., Liang, H.R., Zhao, Y., Liu, X.Q., Sang, L., Chen, R.C., Tang, C.L., Wang, T., Wang, W., He, Q.H., Chen, Z.S., Wong, S.S., Zanin, M., Liu, J., Xu, X., Huang, J., Li, J.F., Ou, L.M., Cheng, B., Xiong, S., Xie, Z.H.,

Ni, Z.Y., Hu, Y., Liu, L., Shan, H., Lei, C.L., Peng, Y.X., Wei, L., Liu, Y., Hu, Y.H., Peng, P., Wang, J.M., Liu, J.Y., Chen, Z., Li, G., Zheng, Z.J., Qiu, S.Q., Luo, J., Ye, C. J., Zhu, S.Y., Cheng, L.L., Ye, F., Li, S.Y., Zheng, J.P., Zhang, N.F., Zhong, N.S., He, J. X., 2020. Clinical characteristics and outcomes of hospitalised patients with COVID-19 treated in Hubei (epicenter) and outside Hubei (non-epicenter): a Nationwide Analysis of China. Eur. Respir. J. 55 (6), 2000562.

Liu, Q., Cheng, S., Chen, R., Ke, J., Liu, Y., Li, Y., Feng, W., Li, F., 2020a. Near-infrared lanthanide-doped nanoparticles for a low interference lateral flow immunoassay test. ACS Appl. Mater. Interfaces 12 (4), 4358–4365.

Liu, C., Geva, E., Mauk, M., Qiu, X., Abrams, W.R., Malamud, D., Curtis, K., Owen, S.M., Bau, H.H., 2011. An isothermal amplification reactor with an integrated isolation membrane for point-of-care detection of infectious diseases. Analyst 136 (10), 2069–2076.

Lippi, G., Simundic, A.M., Plebani, M., 2020. Potential preanalytical and analytical vulnerabilities in the laboratory diagnosis of coronavirus disease 2019 (COVID-19). Clin. Chem. Lab. Med. 58 (7), 1070–1076.

Liu, W., Liu, L., Kou, G., Zheng, Y., Ding, Y., Ni, W., Wang, Q., Tan, L., Wu, W., Tang, S., Xiong, Z., Zheng, S., 2020b. Evaluation of nucleocapsid and spike protein-based ELISAs for detecting antibodies against SARS-CoV-2. J. Clin. Microbiol. 58 (6), e00461.

Loeffelholz, M.J., Tang, Y.W., 2020. Laboratory diagnosis of emerging human coronavirus infections - the state of the art. Emerg. Microb. Infect. 1–26.

Long, Q.X., Liu, B.Z., Deng, H.J., Wu, G.C., Deng, K., Chen, Y.K., Liao, P., Qiu, J.F., Lin, Y., Cai, X.F., Wang, D.Q., Hu, Y., Ren, J.H., Tang, N., Xu, Y.Y., Yu, L.H., Mo, Z., Gong, F., Zhang, X.L., Tian, W.G., Hu, L., Zhang, X.X., Xiang, J.L., Du, H.X., Liu, H. W., Lang, C.H., Luo, X.H., Wu, S.B., Cui, X.P., Zhou, Z., Zhu, M.M., Wang, J., Xue, C. J., Li, X.F., Wang, L., Li, Z.J., Wang, K., Niu, C.C., Yang, Q.J., Tang, X.J., Zhang, Y., Liu, X.M., Li, J.J., Zhang, D.C., Zhang, F., Liu, P., Yuan, J., Li, Q., Hu, J.L., Chen, J., Huang, A.L., 2020. Antibody responses to SARS-CoV-2 in patients with COVID-19. Nat. Med. 26 (6), 845–848.

Lou, B., Li, T., Zheng, S., Su, Y., L, Z., Liu, W., Yu, F., Ge, s., Zou, Q., Yuan, Q., Lin, S., Hong, C., Yao, X., Zhang, X., Wu, D., z, G., Hou, W., Li, T., Zhang, Y., Zhang, S., Fan, J., Zhang, J., Xia, N., Chen, Y., 2020. Serology Characteristics of SARS-CoV-2 Infection since the Exposure and Post Symptoms Onset. medRxiv.

Lu, R., Wu, X., Wan, Z., Li, Y., Jin, X., Zhang, C., 2020a. A novel reverse transcription loop-mediated isothermal amplification method for rapid detection of SARS-CoV-2. Int. J. Mol. Sci. 21 (8), 2826.

Lu, R., Wu, X., Wan, Z., Li, Y., Zuo, L., Qin, J., Jin, X., Zhang, C., 2020b. Development of a novel reverse transcription loop-mediated isothermal amplification method for rapid detection of SARS-CoV-2. Virol. Sin. 35 (3), 344–347.

Lucia, C., Federico, P.-B., Alejandra, G.C., 2020. An Ultrasensitive, Rapid, and Portable Coronavirus SARS-CoV-2 Sequence Detection Method Based on CRISPR-Cas12. bioRxiv.

Lutz, S., Weber, P., Focke, M., Faltin, B., Hoffmann, J., Muller, C., Mark, D., Roth, G., Munday, P., Armes, N., Piepenburg, O., Zengerle, R., von Stetten, F., 2010. Microfluidic lab-on-a-foil for nucleic acid analysis based on isothermal recombinase polymerase amplification (RPA). Lab Chip 10 (7), 887–893.

Lv, L., Xie, X., Gong, Q., Feng, R., Guo, X., Su, B., Chen, L., 2020. Transcriptional Difference between SARS-COV-2 and Other Human Coronaviruses Revealed by Sub-genomic RNA Profiling. bioRxiv.

Ma, Y.D., Li, K.H., Chen, Y.H., Lee, Y.M., Chou, S.T., Lai, Y.Y., Huang, P.C., Ma, H.P., Lee, G.B., 2019. A sample-to-answer, portable platform for rapid detection of pathogens with a smartphone interface. Lab Chip 19 (22), 3804–3814.

Maity, A., Sui, X., Jin, B., Pu, H., Bottum, K.J., Huang, X., Chang, J., Zhou, G., Lu, G., Chen, J., 2018. Resonance-frequency modulation for rapid, point-of-care ebola-glycoprotein diagnosis with a graphene-based field-effect biotransistor. Anal. Chem. 90 (24), 14230–14238.

Mandal, H.S., Su, Z., Ward, A., Tang, X.S., 2012. Carbon nanotube thin film biosensors for sensitive and reproducible whole virus detection. Theranostics 2 (3), 251–257.

Masson, J.F., 2017. Surface plasmon resonance clinical biosensors for medical diagnostics. ACS Sens. 2 (1), 16–30.

Masters, P.S., 2019. Coronavirus genomic RNA packaging. Virology 537, 198–207.

Mauk, M., Song, J., Bau, H.H., Gross, R., Bushman, F.D., Collman, R.G., Liu, C., 2017. Miniaturized devices for point of care molecular detection of HIV. Lab Chip 17 (3), 382–394.

Nalla, A.K., Casto, A.M., Huang, M.W., Perchetti, G.A., Sampoleo, R., Shrestha, L., Wei, Y., Zhu, H., Jerome, K.R., Greninger, A.L., 2020. Comparative performance of SARS-CoV-2 detection assays using seven different primer/probe sets and one assay kit. J. Clin. Microbiol. 58 (6), e00557–20.

Nehra, A., Pal Singh, K., 2015. Current trends in nanomaterial embedded field effect transistor-based biosensor. Biosens. Bioelectron. 74, 731–743.

Neuman, B.W., Adair, B.D., Yoshioka, C., Quispe, J.D., Orca, G., Kuhn, P., Milligan, R.A., Yeager, M., Buchmeier, M.J., 2006. Supramolecular architecture of severe acute respiratory syndrome coronavirus revealed by electron cryomicroscopy. J. Virol. 80 (16), 7918–7928.

Nie, S., Roth, R.B., Stiles, J., Mikhlina, A., Lu, X., Tang, Y.W., Babady, N.E., 2014. Evaluation of Alere i Influenza A&B for rapid detection of influenza viruses A and B. J. Clin. Microbiol. 52 (9), 3339–3344.

Nyan, D.C., Ulitzky, L.E., Cehan, N., Williamson, P., Winkelman, V., Rios, M., Taylor, D. R., 2014. Rapid detection of hepatitis B virus in blood plasma by a specific and sensitive loop-mediated isothermal amplification assay. Clin. Infect. Dis. 59 (1), 16–23.

Oh, J., Yoo, G., Chang, Y.W., Kim, H.J., Jose, J., Kim, E., Pyun, J.C., Yoo, K.H., 2013. A carbon nanotube metal semiconductor field effect transistor-based biosensor for detection of amyloid-beta in human serum. Biosens. Bioelectron. 50, 345–350.

Okba, N.M.A., Muller, M.A., Li, W., Wang, C., GeurtsvanKessel, C.H., Corman, V.M., Lamers, M.M., Sikkema, R.S., de Bruin, E., Chandler, F.D., Yazdanpanah, Y., Le Hingrat, Q., Descamps, D., Houhou-Fidouh, N., Reusken, C., Bosch, B.J., Drosten, C., Koopmans, M.P.G., Haagmans, B.L., 2020. Severe acute respiratory syndrome coronavirus 2-specific antibody responses in coronavirus disease 2019 patients. Emerg. Infect. Dis. 26 (7), 1478–1488.

Okba, N.M.A., Raj, V.S., Widjaja, I., GeurtsvanKessel, C.H., de Bruin, E., Chandler, F.D., Park, W.B., Kim, N.J., Farag, E., Al-Hajri, M., Bosch, B.J., Oh, M.D., Koopmans, M.P. G., Reusken, C., Haagmans, B.L., 2019. Sensitive and specific detection of low-level antibody responses in mild Middle East respiratory syndrome coronavirus infections. Emerg. Infect. Dis. 25 (10), 1868–1877.

Ouyang, W., Han, J., 2019. Universal amplification-free molecular diagnostics by billion-fold hierarchical nanofluidic concentration. Proc. Natl. Acad. Sci. U.S.A. 116 (33), 16240–16249.

Ouyang, W., Han, J., 2020. One-step nucleic acid purification and noise-resistant polymerase chain reaction by electrokinetic concentration for ultralow-abundance nucleic acid detection. Angew. Chem. 59 (27), 10981–10988.

Ouyang, W., Li, Z., Han, J., 2018. Pressure-modulated selective electrokinetic trapping for direct enrichment, purification, and detection of nucleic acids in human serum. Anal. Chem. 90 (19), 11366–11375.

Pan, Y., Long, L., Zhang, D., Yan, T., Cui, S., Yang, P., Wang, Q., Ren, S., 2020b. Potential false-negative nucleic acid testing results for Severe Acute Respiratory Syndrome Coronavirus 2 from thermal inactivation of samples with low viral loads. Clin. Chem.

Pan, L., Mu, M., Yang, P., Sun, Y., Wang, R., Yan, J., Li, P., Hu, B., Wang, J., Hu, C., Jin, Y., Niu, X., Ping, R., Du, Y., Li, T., Xu, G., Hu, Q., Tu, L., 2020a. Clinical characteristics of COVID-19 patients with digestive symptoms in Hubei, China: a descriptive, cross-sectional, multicenter study. Am. J. Gastroenterol.

Park, G.S., Ku, K., Baek, S.H., Kim, S.J., Kim, S.I., Kim, B.T., Maeng, J.S., 2020. Development of reverse transcription loop-mediated isothermal amplification assays targeting SARS-CoV-2. J. Mol. Diagn. : J. Mod. Dynam. 22 (6), 729–735.

Perlman, S., Netland, J., 2009. Coronaviruses post-SARS: update on replication and pathogenesis. Nat. Rev. Microbiol. 7 (6), 439–450.

Phillips, E.A., Moehling, T.J., Bhadra, S., Ellington, A.D., Linnes, J.C., 2018. Strand displacement probes combined with isothermal nucleic acid amplification for instrument-free detection from complex samples. Anal. Chem. 90 (11), 6580–6586.

Phillips, E.A., Moehling, T.J., Ejendal, K.F.K., Hoilett, O.S., Byers, K.M., Basing, L.A., Jankowski, L.A., Bennett, J.B., Lin, L.K., Stanciu, L.A., Linnes, J.C., 2019. Microfluidic rapid and autonomous analytical device (microRAAD) to detect HIV from whole blood samples. Lab Chip 19 (20), 3375–3386.

Qiu, G., Gai, Z., Tao, Y., Schmitt, J., Kullak-Ublick, G.A., Wang, J., 2020. Dual-functional plasmonic photothermal biosensors for highly accurate severe acute respiratory syndrome coronavirus 2 detection. ACS Nano 14 (5), 5268–5277.

Qu, J., Wu, C., Li, X., Zhang, G., Jiang, Z., Li, X., Zhu, Q., Liu, L., 2020. Profile of IgG and IgM antibodies against severe acute respiratory syndrome coronavirus 2 (SARS-CoV-2). Clin. Infect. Dis. ciaa489.

Qu, Y., Marshall, L.A., Santiago, J.G., 2014. Simultaneous purification and fractionation of nucleic acids and proteins from complex samples using bidirectional isotachophoresis. Anal. Chem. 86 (15), 7264–7268.

Ramnani, P., Gao, Y., Ozsoz, M., Mulchandani, A., 2013. Electronic detection of microRNA at attomolar level with high specificity. Anal. Chem. 85 (17), 8061–8064.

Rauch, J.N., Valois, E., Solley, S.C., Braig, F., Lach, R.S., Baxter, N.J., Kosik, K.S., Arias, C., Acosta-Alvear, D., Wilson, M.Z., 2020. A Scalable, Easy-To-Deploy, Protocol for Cas13-Based Detection of SARS-CoV-2 Genetic Material. bioRxiv.

Reboud, J., Xu, G., Garrett, A., Adriko, M., Yang, Z., Tukahebwa, E.M., Rowell, C., Cooper, J.M., 2019. Paper-based microfluidics for DNA diagnostics of malaria in low resource underserved rural communities. Proc. Natl. Acad. Sci. U.S.A. 116 (11), 4834–4842.

Rhoads, D.D., Cherian, S.S., Roman, K., Stempak, L.M., Schmotzer, C.L., Sadri, N., 2020. Comparison of Abbott ID Now, Diasorin Simplexa, and CDC FDA EUA methods for the detection of SARS-CoV-2 from nasopharyngeal and nasal swabs from individuals diagnosed with COVID-19. J. Clin. Microbiol. JCM.00760–20.

Rogacs, A., Marshall, L.A., Santiago, J.G., 2014. Purification of nucleic acids using isotachophoresis. J. Chromatogr., A 1335, 105–120.

Rota, P.A., Oberste, M.S., Monroe, S.S., Nix, W.A., Campagnoli, R., Icenogle, J.P., Penaranda, S., Bankamp, B., Maher, K., Chen, M.H., Tong, S., Tamin, A., Lowe, L., Frace, M., DeRisi, J.L., Chen, Q., Wang, D., Erdman, D.D., Peret, T.C., Burns, C., Ksiazek, T.G., Rollin, P.E., Sanchez, A., Liffick, S., Holloway, B., Limor, J., McCaustland, K., Olsen-Rasmussen, M., Fouchier, R., Gunther, S., Osterhaus, A.D., Drosten, C., Pallansch, M.A., Anderson, L.J., Bellini, W.J., 2003. Characterization of a novel coronavirus associated with severe acute respiratory syndrome. Science 300 (5624), 1394–1399.

Sawicki, S.G., Sawicki, D.L., Siddell, S.G., 2007. A contemporary view of coronavirus transcription. J. Virol. 81 (1), 20–29.

Schoeman, D., Fielding, B.C., 2019. Coronavirus envelope protein: current knowledge. Virol. J. 16 (1), 69.

Seo, G., Lee, G., Kim, M.J., Baek, S.H., Choi, M., Ku, K.B., Lee, C.S., Jun, S., Park, D., Kim, H.G., Kim, S.J., Lee, J.O., Kim, B.T., Park, E.C., Kim, S.I., 2020. Rapid detection of COVID-19 causative virus (SARS-CoV-2) in human nasopharyngeal swab specimens using field-effect transistor-based biosensor. ACS Nano 14 (4), 5135–5142.

Shen, Z., Xiao, Y., Kang, L., Ma, W., Shi, L., Zhang, L., Zhou, Z., Yang, J., Zhong, J., Yang, D., Guo, L., Zhang, G., Li, H., Xu, Y., Chen, M., Gao, Z., Wang, J., Ren, L., Li, M., 2020. Genomic diversity of SARS-CoV-2 in coronavirus disease 2019 patients. Clin. Infect. Dis. ciaa203.

Son, M., Kim, D., Park, K.S., Hong, S., Park, T.H., 2016. Detection of aquaporin-4 antibody using aquaporin-4 extracellular loop-based carbon nanotube biosensor for the diagnosis of neuromyelitis optica. Biosens. Bioelectron. 78, 87–91.
Steinmetz, M., Lima, D., Viana, A.G., Fujiwara, S.T., Pessoa, C.A., Etto, R.M., Wohnrath, K., 2019. A sensitive label-free impedimetric DNA biosensor based on silsesquioxane-functionalized gold nanoparticles for Zika Virus detection. Biosens. Bioelectron. 141, 111351.
Subramanian Parimalam, S., Oguchi, Y., Abdelmoez, M.N., Tsuchida, A., Ozaki, Y., Yokokawa, R., Kotera, H., Shintaku, H., 2018. Electrical lysis and RNA extraction from single cells fixed by dithiobis(succinimidyl propionate). Anal. Chem. 90 (21), 12512–12518.
Sun, B., Feng, Y., Mo, X., Zheng, P., Wang, Q., Li, P., Peng, P., Liu, X., Chen, Z., Huang, H., Zhang, F., Luo, W., Niu, X., Hu, P., Wang, L., Peng, H., Huang, Z., Feng, L., Li, F., Zhang, F., Li, F., Zhong, N., Chen, L., 2020. Kinetics of SARS-CoV-2 specific IgM and IgG responses in COVID-19 patients. Emerg. Microb. Infect. 1–36.
Tian, X., Li, C., Huang, A., Xia, S., Lu, S., Shi, Z., Lu, L., Jiang, S., Yang, Z., Wu, Y., Ying, T., 2020. Potent binding of 2019 novel coronavirus spike protein by a SARS coronavirus-specific human monoclonal antibody. Emerg. Microb. Infect. 9 (1), 382–385.
To, K.K., Tsang, O.T., Leung, W.S., Tam, A.R., Wu, T.C., Lung, D.C., Yip, C.C., Cai, J.P., Chan, J.M., Chik, T.S., Lau, D.P., Choi, C.Y., Chen, L.L., Chan, W.M., Chan, K.H., Ip, J.D., Ng, A.C., Poon, R.W., Luo, C.T., Cheng, V.C., Chan, J.F., Hung, I.F., Chen, Z., Chen, H., Yuen, K.Y., 2020. Temporal profiles of viral load in posterior oropharyngeal saliva samples and serum antibody responses during infection by SARS-CoV-2: an observational cohort study. Lancet Infect. Dis. 20 (5), 565–574.
Wang, C.H., Lien, K.Y., Wang, T.Y., Chen, T.Y., Lee, G.B., 2011. An integrated microfluidic loop-mediated-isothermal-amplification system for rapid sample pre-treatment and detection of viruses. Biosens. Bioelectron. 26 (5), 2045–2052.
Wang, W., Xu, Y., Gao, R., Lu, R., Han, K., Wu, G., Tan, W., 2020. Detection of SARS-CoV-2 in different types of clinical specimens. JAMA 323 (18), 1843–1844.
Wei, W.E., Li, Z., Chiew, C.J., Yong, S.E., Toh, M.P., Lee, V.J., 2020. Presymptomatic transmission of SARS-CoV-2 - Singapore, January 23-March 16, 2020. MMWR (Morb. Mortal. Wkly. Rep.) 69 (14), 411–415.
Woo, P.C., Lau, S.K., Wong, B.H., Tsoi, H.W., Fung, A.M., Kao, R.Y., Chan, K.H., Peiris, J. S., Yuen, K.Y., 2005. Differential sensitivities of severe acute respiratory syndrome (SARS) coronavirus spike polypeptide enzyme-linked immunosorbent assay (ELISA) and SARS coronavirus nucleocapsid protein ELISA for serodiagnosis of SARS coronavirus pneumonia. J. Clin. Microbiol. 43 (7), 3054–3058.
Woo, P.C.Y., Lau, S.K.P., Chen, Y., Wong, E.Y.M., Chan, K.H., Chen, H., Zhang, L., Xia, N., Yuen, K.Y., 2018. Rapid detection of MERS coronavirus-like viruses in bats: pote1ntial for tracking MERS coronavirus transmission and animal origin. Emerg. Microb. Infect. 7 (1), 18.
Wyllie, A.L., Fournier, J., Massana, A., Campbell, M., Tokuyama, M., Vijayakumar, P., Geng, B., Muenker, M.C., Moore, A.J., Vogels, C.B.F., Petrone, M.E., Ott, I.M., Lu, P., Culligan, A.L., Klein, J., Venkataraman, A., Earnest, R., Simonov, M., Datta, R., Handoko, R., Naushad, N., Sewanan, L.R., Valdez, J., White, E.B., Lapidus, S., Kalinich, C.C., Jiang, X., Kim, D.J., Kudo, E., Linehan, M., Mao, T., Moriyama, M., Oh, J.E., Park, A., Silva, J., Song, E., Takahashi, T., Taura, M., Weizman, O.-E., Wong, P., Yang, Y., Bermejo, S., Odio, C., Omer, S.B., Cruz, C.S.D., Farhadian, S., Martinello, R.A., Iwasaki, A., Grubaugh, N.D., Ko, A.I., 2020. Saliva Is More Sensitive for SARS-CoV-2 Detection in COVID-19 Patients than Nasopharyngeal Swabs. medRxiv.
Xie, C., Jiang, L., Huang, G., Pu, H., Gong, B., Lin, H., Ma, S., Chen, X., Long, B., Si, G., Yu, H., Jiang, L., Yang, X., Shi, Y., Yang, Z., 2020a. Comparison of different samples for 2019 novel coronavirus detection by nucleic acid amplification tests. Int. J. Infect. Dis. IJID 93, 264–267.
Xie, X., Zhong, Z., Zhao, W., Zheng, C., Wang, F., Liu, J., 2020b. Chest CT for typical 2019-nCoV pneumonia: relationship to negative RT-PCR testing. Radiology 296 (2), E41–E45.
Yan, C., Cui, J., Huang, L., Du, B., Chen, L., Xue, G., Li, S., Zhang, W., Zhao, L., Sun, Y., Yao, H., Li, N., Zhao, H., Feng, Y., Liu, S., Zhang, Q., Liu, D., Yuan, J., 2020. Rapid and visual detection of 2019 novel coronavirus (SARS-CoV-2) by a reverse transcription loop-mediated isothermal amplification assay. Clin. Microbiol. Infect. 26 (6), 773–779.
Yang, H., Chen, Z., Cao, X., Li, Z., Stavrakis, S., Choo, J., deMello, A.J., Howes, P.D., He, N., 2018. A sample-in-digital-answer-out system for rapid detection and quantitation of infectious pathogens in bodily fluids. Anal. Bioanal. Chem. 410 (27), 7019–7030.
Yeh, C.H., Kumar, V., Moyano, D.R., Wen, S.H., Parashar, V., Hsiao, S.H., Srivastava, A., Saxena, P.S., Huang, K.P., Chang, C.C., Chiu, P.W., 2016. High-performance and high-sensitivity applications of graphene transistors with self-assembled monolayers. Biosens. Bioelectron. 77, 1008–1015.
Yehia, N., Arafa, A.S., Abd El Wahed, A., El-Sanousi, A.A., Weidmann, M., Shalaby, M.A., 2015. Development of reverse transcription recombinase polymerase amplification assay for avian influenza H5N1 HA gene detection. J. Virol Methods 223, 45–49.
Yin, J., Zou, Z., Hu, Z., Zhang, S., Zhang, F., Wang, B., Lv, S., Mu, Y., 2020. A "sample-in-multiplex-digital-answer-out" chip for fast detection of pathogens. Lab Chip 20 (5), 979–986.
Yip, C.C., Ho, C.C., Chan, J.F., To, K.K., Chan, H.S., Wong, S.C., Leung, K.H., Fung, A.Y., Ng, A.C., Zou, Z., Tam, A.R., Chung, T.W., Chan, K.H., Hung, I.F., Cheng, V.C., Tsang, O.T., Tsui, S.K.W., Yuen, K.Y., 2020. Development of a novel, genome subtraction-derived, SARS-CoV-2-specific COVID-19-nsp2 real-time RT-PCR assay and its evaluation using clinical specimens. Int. J. Mol. Sci. 21 (7), 2574.
Zhang, H., Miller, B.L., 2019. Immunosensor-based label-free and multiplex detection of influenza viruses: state of the art. Biosens. Bioelectron. 141, 111476.
Yu, F., Yan, L., Wang, N., Yang, S., Wang, L., Tang, Y., Gao, G., Wang, S., Ma, C., Xie, R., Wang, F., Tan, C., Zhu, L., Guo, Y., Zhang, F., 2020a. Quantitative Detection and Viral Load Analysis of SARS-CoV-2 in Infected Patients. Clinical Infectious Diseases. an official publication of the Infectious Diseases Society of America.
Yu, P., Zhu, J., Zhang, Z., Han, Y., Huang, L., 2020b. A familial cluster of infection associated with the 2019 novel coronavirus indicating potential person-to-person transmission during the incubation period. J. Infect. Dis.
Zhang, J., Liu, J., Li, N., Liu, Y., Ye, R., Qin, X., Zheng, R., 2020. Serological Detection of 2019-nCoV Respond to the Epidemic: A Useful Complement to Nucleic Acid Testing. medRxiv.
Zhang, Y., Odiwuor, N., Xiong, J., Sun, L., Nyaruaba, R.O., Wei, H., Tanner, N.A., 2020. Rapid Molecular Detection of SARS-CoV-2 (COVID-19) Virus RNA Using Colorimetric LAMP. medRxiv.
Zhao, J., Yuan, Q., Wang, H., Liu, W., Liao, X., Su, Y., Wang, X., Yuan, J., Li, T., Li, J., Qian, S., Hong, C., Wang, F., Liu, Y., Wang, Z., He, Q., Li, Z., He, B., Zhang, T., Fu, Y., Ge, S., Liu, L., Zhang, J., Xia, N., Zhang, Z., 2020. Antibody responses to SARS-CoV-2 in patients of novel coronavirus disease 2019. Clin. Infect. Dis. 28 ciaa344.
Zhou, P., Yang, X.L., Wang, X.G., Hu, B., Zhang, L., Zhang, W., Si, H.R., Zhu, Y., Li, B., Huang, C.L., Chen, H.D., Chen, J., Luo, Y., Guo, H., Jiang, R.D., Liu, M.Q., Chen, Y., Shen, X.R., Wang, X., Zheng, X.S., Zhao, K., Chen, Q.J., Deng, F., Liu, L.L., Yan, B., Zhan, F.X., Wang, Y.Y., Xiao, G.F., Shi, Z.L., 2020. A pneumonia outbreak associated with a new coronavirus of probable bat origin. Nature 579 (7798), 270–273.
Zhu, H., Fohlerova, Z., Pekarek, J., Basova, E., Neuzil, P., 2020. Recent advances in lab-on-a-chip technologies for viral diagnosis. Biosens. Bioelectron. 153, 112041.